AD-A168 999 THE APPLICATION OF BOUNDARY-ELEMENT TECHNIQUES FOR SOME SOIL-STRUCTURE IN.. (U) TEXAS TECH UNIV LUBBOCK DEPT OF CIVIL ENGINEERING C V VALLABHAN ET AL. APR 86 ATC-86-2 1/1

UNCLASSIFIED DACW39-83-M-1805 F/G 8/13 NL

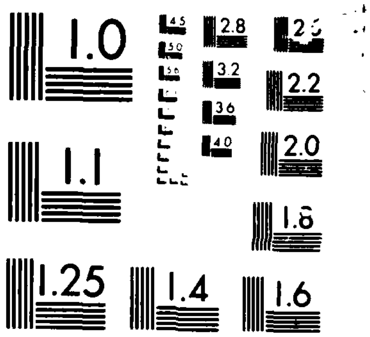
1.0
1.1
1.25
1.4
1.6
1.8
2.0
2.2
2.8
3.2
3.6
4.0
4.5
5.0

12

TECHNICAL REPORT ATC-86-2

THE APPLICATION OF BOUNDARY-ELEMENT TECHNIQUES FOR SOME SOIL-STRUCTURE INTERACTION PROBLEMS

by

C. V. Girija Vallabhan, Jayaraman Sivakumar

Department of Civil Engineering
Texas Tech University
Lubbock, Texas 79409

April 1986

Final Report

DEPARTMENT OF THE ARMY
US Army Corps of Engineers
Washington, DC 20314-1000

Contract No. DACW39-83-M-1805

Automation Technology Center
US Army Engineer Waterways Experiment Station
PO Box 631, Vicksburg, Mississippi 39180-0631

Destroy this report when no longer needed. Do not return it to the originator.

The findings in this report are not to be construed as an official Department of the Army position unless so designated by other authorized documents.

Unclassified

SECURITY CLASSIFICATION OF THIS PAGE (When Data Entered)

REPORT DOCUMENTATION PAGE		READ INSTRUCTIONS BEFORE COMPLETING FORM
1. REPORT NUMBER Technical Report ATC-86-2	2. GOVT ACCESSION NO. AD-A168 999	3. RECIPIENT'S CATALOG NUMBER
4. TITLE (and Subtitle) THE APPLICATION OF BOUNDARY-ELEMENT TECHNIQUES FOR SOME SOIL-STRUCTURE INTERACTION PROBLEMS		5. TYPE OF REPORT & PERIOD COVERED Final report 6. PERFORMING ORG. REPORT NUMBER
7. AUTHOR(s) C. V. Girija Vallabhan Jayaraman Sivakumar		8. CONTRACT OR GRANT NUMBER(s) Contract No. DACW39-83-M-1805
9. PERFORMING ORGANIZATION NAME AND ADDRESS Texas Tech University Department of Civil Engineering Lubbock, Texas 79409		10. PROGRAM ELEMENT, PROJECT, TASK AREA & WORK UNIT NUMBERS
11. CONTROLLING OFFICE NAME AND ADDRESS DEPARTMENT OF THE ARMY US Army Corps of Engineers Washington, DC 20314-1000		12. REPORT DATE April 1986 13. NUMBER OF PAGES 87
14. MONITORING AGENCY NAME & ADDRESS(if different from Controlling Office) US Army Engineer Waterways Experiment Station Automation Technology Center PO Box 631, Vicksburg, Mississippi 39180-0631		15. SECURITY CLASS. (of this report) Unclassified 15a. DECLASSIFICATION DOWNGRADING SCHEDULE

16. DISTRIBUTION STATEMENT (of this Report)

Approved for public release; distribution unlimited.

17. DISTRIBUTION STATEMENT (of the abstract entered in Block 20, if different from Report)

18. SUPPLEMENTARY NOTES

Available from National Technical Information Service, 5285 Port Royal Road, Springfield, Virginia 22161.

19. KEY WORDS (Continue on reverse side if necessary and identify by block number)

Soil mechanics--Mathematics (LC)
Soil-structure interaction (WES)
Structural engineering--Mathematics (LC)

20. ABSTRACT (Continue on reverse side if necessary and identify by block number)

Boundary-element technique research performed to solve soil-structure interaction problems is the basis for this report. Specifically, it was designed to answer questionable situations for long hydraulic U-Lock structures erected on elastic soil. An assembling of facts from an earlier research that employed the Kelvin-type element directed the decision in favor of Flamant-type boundary element. Both constant and linear elements were

(Continued)

DD FORM 1473 1 JAN 73 EDITION OF 1 NOV 65 IS OBSOLETE

Unclassified

SECURITY CLASSIFICATION OF THIS PAGE (When Data Entered)

20. ABSTRACT (Continued).

developed and numerous sample problems were dealt with to illustrate the capabilities of these elements in the problem situations of soil-structure relationships.

When research was finalized the Flamant-type boundary element proved to be convenient, gave better results for displacement problems using the constant element, offered satisfactory behavior description of soil-structure response, required considerably fewer elements than the conventional model, provided more accuracy in stress analysis of structure, and was confirmed as very beneficial for use in input data preparation.

This study concentrated further on research into soil-structure interaction problems with the structure modeled by the finite-element method and the soil modeled by the boundary-element method.

A model problem suggested by the US Army Engineer Waterways Experiment Station was selected for study and solving. The emphasis of this research was to develop a convenient and economical technique to couple the boundary- and finite-element methods of analysis to accomplish the investigation.

A computer code for the coupling of the two methods have been developed in FORTRAN.

PREFACE

This report presents investigations and results of the boundary- and finite-element techniques for solving soil-structure interaction problems. With the boundary-element method used for modeling the soil and the finite-element method used as the structure model, a coupling technique of the two methods was instrumented. The project was funded by the Civil Works Research and Development Program of the Office, Chief of Engineers, US Army (OCE), under the Structural Engineering Research Program work unit of the Soil-Structure Interaction (SSI) Studies Project.

Development of a computer program was accomplished and the report was written by Dr. C. V. Girija Vallabhan and Dr. Jayaraman Sivakumar, Department of Civil Engineering, Texas Tech University, Lubbock, Texas, under Contract No. DACW39-83-M-1805 with the US Army Engineer Waterways Experiment Station (WES), Vicksburg, Miss.

Dr. N. Radhakrishnan, Automation Technology Center (ATC), WES, and SSI Studies Project Manager, coordinated and monitored the work. Dr. Radhakrishnan was Special Technical Assistant, ATC, at the initiation of the work and Chief of the Center during publication of the report. Dr. Robert Hall aided in the coordination and monitoring of the work. This report was edited by Mrs. Gilda Shurden, Publications and Graphic Arts Division, WES. Mr. Donald R. Dressler was the point of contact in OCE.

COL Allen F. Grum, USA, was Director of WES during the publication of the report. Technical Director was Dr. Robert W. Whalin.

CONTENTS

CONVERSION FACTORS, NON-SI TO SI (METRIC) UNITS OF MEASUREMENT

Non-SI units of measurement used in this report can be converted to SI (metric) units as follows:

Multiply	By	To Obtain
feet	0.3048	metres
kips (force)	4.448222	kilonewtons
kip (force)-feet	1355.818	newton-metres
kips (force) per square inch	6.894757	megapascals
pounds (force) per square inch	6.894757	kilopascals

THE APPLICATION OF BOUNDARY-ELEMENT TECHNIQUES FOR SOME SOIL-STRUCTURE INTERACTION PROBLEMS

PART I: PROBLEMS AND SOLUTIONS

Introduction

1. Soil-structure interaction problems result when the behavior of the structure and the surrounding soil are interdependent, and the solution requires an analysis of both the structure and the soil in a compatible manner. While structures are often satisfactorily modeled as linearly elastic, homogeneous, and isotropic materials, the modeling of soils is extremely complex. To model the in-situ behavior of soils, one must make gross approximations by using experience and judgment, and these evaluations are chiefly based on the relative importance of the project and the desired accuracy. The complexities in the constitutive relations of the soil continuum are enhanced by the fact that the soil has been deposited in nature in a layered, heterogeneous manner. Since, in most instances, engineers are interested only in the behavior of structures, they have assumed very simplified properties of the soil in their design considerations. One of the widely used models for soil-structure interaction problems is the Winkler spring model (Scott 1981) for analysis of beams on elastic foundations, mat foundations, pavements, pile foundations, etc.

Winkler Model

2. Winkler, in 1867, proposed that the deflection of the soil surface can be modeled by a simple equation,*

$$p = kw \tag{1}$$

where

p = the pressure acting on the soil surface

k = the proportionality constant, known as the subgrade modulus or the modulus of subgrade reaction

w = the deflection of the loaded region on the surface

---

* For convenience, symbols and abbreviations are listed in the Notation (Appendix D).

The unit of k is in pounds per cubic inch. Normally, simple plate bearing tests are conducted to determine the value of k . This concept has been widely used by engineers. For a given value of k , Hetenyi (1946) solved many problems of beams on elastic foundation, and Westergaard (1926) solved problems of slabs on elastic foundations. When the question of the value of k of soil was raised, Terzaghi (1955) offered general guidelines. Matlock and Reese (1960) have widely used this technique for solving problems of laterally loaded pile foundations. Terzaghi showed that though linearly elastic, isotropic, and homogeneous properties for soil were used, the modulus of subgrade reaction depended very much on the size of the loaded area. Vesic (1961) showed that the value of k is influenced by the stiffness of the beam. Based on experiments and theoretical concepts, many empirical formulas arose for values of k . These are always questioned by structural engineers who generally demand a soil value of k for their input for the soil-structure-interaction analysis. The absence of a unique value for k for soil can be easily realized from the following examples, even though one assumes idealized properties such as linear, elastic, etc., for the soil continuum.

Example Problem

3. Consider a plane-strain problem with a strip of uniformly loaded beam resting on a semi-infinite soil continuum. If the beam is very rigid as compared to the soil, the deflections along the beam are uniform while the pressure distribution varies from infinity to a finite value at the center. This is shown in Figure 1. On the other hand, if the beam has very low rigidity its deflections vary from a maximum value at the center to a smaller value at the ends, as shown in Figure 2. In each case, the ratio of pressure versus deflection is not a constant at the soil-structure interface, hence the non-uniqueness of the value of k is demonstrated here. Realizing these problems, Pasternak (1954) developed a two-parameter model to take into consideration the end effects. The evaluation of these parameters, however, again becomes a major problem confronting the geotechnical engineer. In addition, it can be shown that the value of k depends on the depth of the soil continuum; in other words, it is influenced by the existence of hard-rock stratum and the depth at which it occurs.

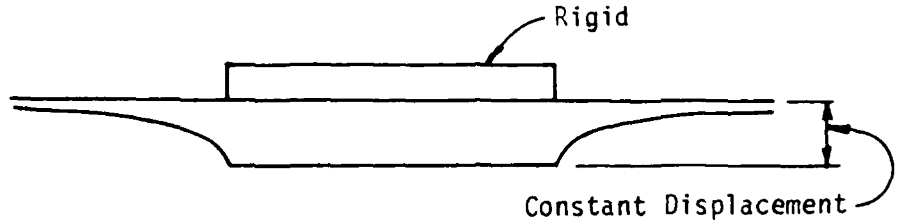

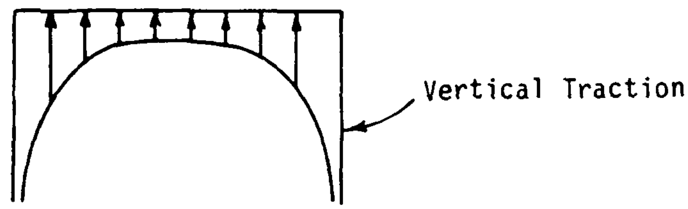

Figure 1. Pressure distribution on the interface of a rigid beam

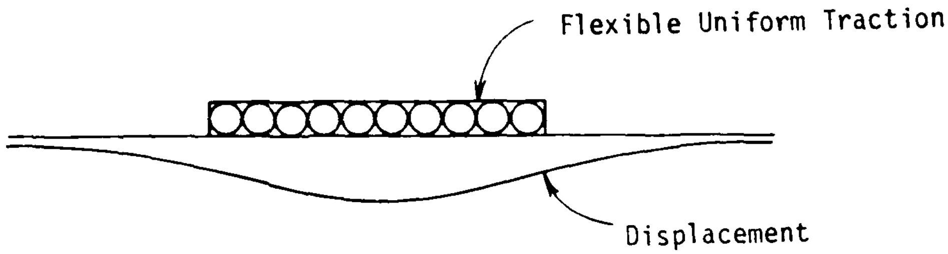

Figure 2. Deflection on the interface of a flexible beam

4. In spite of these limitations, the concept of the constant, or even nonlinear, k is used by engineers for analysis of moderately simple structures. However, when these concepts are applied to analysis of major structures, such as hydraulic U-lock structures, a better and more accurate determination of the soil stiffness based on its constitutive relations is necessary.

Alternate Methods

5. An alternate and better method of analysis is to model the involved soil continuum in its entirety. Closed form mathematical solutions to achieve

this become too tedious, even for relatively simple problems. However, electronic computers made it possible to analyze these problems numerically, by using methods such as finite difference, finite element, etc. Researchers, Duncan and Clough (1971) and Vallabhan and Jain (1972) have used finite-element methods (FEM) for solving soil-structure interaction problems. These methods become cumbersome as the number of unknowns increases rapidly, and more so when the discretizations of the continuum are altered for more accurate representations of the soil continuum. Normal discretizations of the soil and the structure result in a fairly coarse discretization for the structure. It is in this context that the boundary-element method (BEM) is found advantageous in the analysis of soil-structure interaction problems.

6. Two-dimensional continuum problems are represented at the boundary as line elements and three-dimensional problems are modeled by the boundary surface as surface elements, i.e., BEM, offer a reduction in the dimensionality of the problem. It is found to be an elegant procedure for handling large soil continuum with elements required only on the boundaries, hence, attractive to the analyst.

Capabilities of the Boundary-Element Method

7. Engineers are seeking parameters to represent the soil stiffness underneath the structure, with simple and reasonable assumptions on the soil properties such as Young's modulus E and Poisson's ratio ν of the soil medium. Using the BEM, the stiffness parameters can be developed in a matrix form, without depending on the stiffness of the structure, size of the soil-structure interface area, and the distribution of the loading. The emphasis of this research report is to investigate the boundary-element techniques to represent a soil medium in such a manner that the engineer can more accurately use it in his soil-structure interaction problems.

Mathematical Aspects

8. The mathematical aspects of this technique are given in detail in Part II. Presented here is an overall view of the method, highlighting its advantages over domain-type solutions. The dimensionality of the problem is reduced by one, because the boundary of the domain alone is discretized for

analysis. Therefore, the input data is highly simplified, reducing man hours in preparation of data. Modeling of domains extending to large distances are carried out very efficiently. Moreover, this method, when applied to a stress-concentration problem, yields accurate results when compared to other numerical methods. The only disadvantage is that the system matrix is fully populated and numerical efficiency is not great for slender regions, unless the domain is divided into regions to get a banded type matrix. Overall, the accuracy and efficiency of the model is much higher than those of the other prevailing methods for soil structure interaction problems.

Various Methods Used

9. In this report, the FEM is used for representing the U-lock structure, and the BEM is used for modeling the soil. Rectangular plane-strain elements are used for the structure in the FEM. The boundary of the soil medium is discretized as constant boundary elements. Using a static-condensation procedure, the boundary-element system equations are reduced to the unknown displacements on the soil-structure interface. The stiffness of the soil system is thus developed on the interface and added to the finite-element structure stiffness matrix. The resulting global stiffness is solved for stresses and displacements of the structure, including the interface. The pressure distribution on the interface is then calculated from the boundary-element equations, using the interface displacements. Part III discusses the theory of the coupling technique of the two methods along with the difficulties that can be encountered and ways of circumventing them.

10. Part IV gives the details of the example problem solved to validate the computer code developed. The results are presented in a tabular form and a few cases are compared in the complete finite-element version. Discussion of the results and conclusions is presented in Part V. On the whole, this procedure is found to be very effective and efficient and offers greater potential, particularly in solving hydraulic U-lock structure problems. The model offers capability in representing large linearly elastic soil media in solving complex soil-structure interaction problems with considerable ease in input-data preparation. Finally, recommendations for future work are listed.

PART II: BOUNDARY-ELEMENT METHOD

Introduction

11. This part deals with the basic theory of the BEM. Equations of linear theory of elasticity which are required in the derivation of the boundary-element equations are also presented briefly. The sequence used in the derivation is for the direct method wherein one uses a fundamental solution due to Kelvin (Love 1927). Other simplified boundary element techniques using Flamant equations (Crouch and Starfield 1983) are also investigated; details of this method were gathered in a preliminary study of the material herein. The boundary-element equations are derived in such a form that they can be applied to plane elasticity problems or three-dimensional elasticity problems. The difference will be in the use of corresponding fundamental solutions.

Basic Equations of Elasticity

12. The basic equations of elasticity are presented here for a three-dimensional case. Index notation is used for convenience. The equilibrium equations at any point in the interior domain Ω of a solid continuum are

$$\sigma_{ij,j} + b_i = 0 \quad \text{in} \quad \Omega \tag{2}$$

where

σ_{ij} = stress tensor
b_i = body force vector

The comma after ij represents differentiation of the stress tensor σ_{ij} with respect to the corresponding axes represented by the subscript following the comma.

13. The stress tensor has to match with the prescribed tractions $\tilde{t}_i$ on the boundary, i.e.,

$$\sigma_{ij} n_j = \tilde{t}_i \tag{3}$$

where n_j is the unit normal vector on the boundary Γ_1. Displacements are prescribed on boundary Γ_2,

$$u_i = \tilde{u}_i \quad \text{on} \quad \Gamma_2 \tag{4}$$

In this case, the total boundary $\Gamma = \Gamma_1 + \Gamma_2$. Equations 2, 3, and 4 become the fundamental equations in elasticity. But to solve these equations, one needs two additional sets of equations: one set to represent strain-displacement relationships, i.e.,

$$\varepsilon_{ij} = \frac{1}{2} (u_{i,j} + u_{j,i}) \tag{5}$$

where ε_{ij} is the linear strain tensor, and the second set to represent the stress strain relations, i.e.,

$$\sigma_{ij} = C_{ijkl}\varepsilon_{kl} \tag{6}$$

where C_{ijkl} is a fourth-order material property tensor.

Equations for Boundary-Element Method

14. The derivation of the BEM can be achieved in different ways. Brebbia and Walker (1972) have used a weighted residual approach for derivation of the boundary-element equations. The approach used here differs slightly and is more rational. If u_i^* is assumed as a weighting function, then the equilibrium equation can be written as

$$\int_\Omega (\sigma_{ij,j} + b_i)\, u_i^*\, d\Omega = 0 \tag{7}$$

Considering the integral shown in Equation 8,

$$\int_\Omega (\sigma_{ij}u_i^*)_{,j}\, d\Omega \tag{8}$$

and differentiating the integrand in the above equation,

$$\int_\Omega (\sigma_{ij}u_i^*)_{,j}\, d\Omega = \int_\Omega (\sigma_{ij,j}u_i^*)\, d\Omega + \int_\Omega \sigma_{ij}u_{i,j}^*\, d\Omega \tag{9}$$

By using the divergence theorem and substitution in Equation 3, the results are

$$\begin{aligned} \int_\Omega (\sigma_{ij}u_i^*)_{,j}\, d\Omega &= \int_\Gamma (\sigma_{ij}u_i^*)n_j\, d\Gamma \\ &= \int_\Gamma t_i u_i^*\, d\Gamma \end{aligned} \tag{10}$$

The substitution of Equation 10 into Equation 9 and rearranging Equation 9 into the form of equilibrium Equation 7 results in

$$\int_\Gamma t_i u_i^*\, d\Gamma - \int_\Omega \sigma_{ij}u_{i,j}^*\, d\Omega + \int_\Omega b_i u_i^*\, d\Omega = 0 \tag{11}$$

By using symmetry of stress tensor, i.e., $\sigma_{ij} = \sigma_{ji}$,

$$\begin{aligned} \int_\Omega \sigma_{ij}u_{i,j}^*\, d\Omega &= \int_\Omega \sigma_{ij}\, \frac{1}{2}(u_{i,j}^* + u_{j,i}^*)\, d\Omega \\ &= \int_\Omega \sigma_{ij}\varepsilon_{ij}^*\, d\Omega \end{aligned} \tag{12}$$

The substitution of Equation 12 into Equation 7 results in

$$\int_\Gamma t_i u_i^*\, d\Gamma - \int_\Omega \sigma_{ij}\varepsilon_{ij}^*\, d\Omega + \int_\Omega b_i u_i^*\, d\Omega = 0 \tag{13}$$

By using the stress-strain relationship of Equation 6,

$$\begin{aligned} \int_\Omega \sigma_{ij}\varepsilon_{ij}^*\, d\Omega &= \int_\Omega C_{ijkl}\varepsilon_{kl}\varepsilon_{ij}^*\, d\Omega \\ &= \int_\Omega \sigma_{kl}^*\varepsilon_{kl}\, d\Omega \end{aligned} \tag{14}$$

Following Equation 9,

$$\int_\Omega (\overset{*}{\sigma}_{ij} u_i)_{,j} \, d\Omega = \int_\Omega \overset{*}{\sigma}_{ij,j} u_i \, d\Omega + \int_\Omega \overset{*}{\sigma}_{ij} \varepsilon_{ij} \, d\Omega \tag{15}$$

Following Equation 10, the results are

$$\begin{aligned} \int_\Omega (\overset{*}{\sigma}_{ij} u_i)_{,j} \, d\Omega &= \int_\Gamma \overset{*}{\sigma}_{ij} u_i n_j \, d\Gamma \\ &= \int_\Omega \overset{*}{t}_i u_i \, d\Gamma \end{aligned} \tag{16}$$

Substitution of Equation 16 into Equation 15 and using Equation 14 gives

$$\int_\Gamma \overset{*}{t}_i u_i \, d\Gamma = \int_\Omega \overset{*}{\sigma}_{ij,j} u_i \, d\Omega + \int_\Omega \overset{*}{\sigma}_{ij} \varepsilon_{ij} \, d\Omega \tag{17}$$

Eliminating the second integral on the right-hand side of Equation 17 by using Equation 13 results in

$$\int_\Gamma t_i \overset{*}{u}_i \, d\Gamma - \int_\Gamma \overset{*}{t}_i u_i \, d\Gamma + \int_\Omega \overset{*}{\sigma}_{ij,j} u_i \, d\Omega + \int_\Omega b_i \overset{*}{u}_i \, d\Omega = 0 \tag{18}$$

This is the governing equation for the domain under consideration. The first domain integral in the above equation can be removed by assuming a solution of an equation such that

$$\overset{*}{\sigma}_{ij,j} + \Delta_{il} \, (s \, , \, q) = 0 \quad \text{in} \quad \Omega \tag{19}$$

where

s = source point where a unit load is applied in the l direction

q = field point where the displacements and tractions are calculated due to the unit load

Mathematically,

if $s \neq q$, $\Delta_{il} = 0$;

if $s = q$, and $i = 1$, $\int_\Omega \Delta_{il} \, d\Omega = 1$,

and

if $i \neq 1$; $\Delta_{il} = 0$

The solutions to the above equation u^*_{il} and t^*_{il} for $l = 1, 2, 3$ represent the displacements and tractions in the i direction due to a unit concentrated load at s in the l direction. Substituting Equation 19 into Equation 18, for any source point s , gives

$$-u_l(s) + \int_\Gamma u^*_{lk} t_k \, d\Gamma - \int_\Gamma t^*_{lk} u_k \, d\Gamma + \int_\Omega u^*_{lk} b_k \, d\Omega = 0 \tag{20}$$

Omission of body forces leaves

$$u_l(s) + \int_\Gamma t^*_{lk} u_k \, d\Gamma = \int_\Gamma u^*_{lk} t_k \, d\Gamma \tag{21}$$

Equation 21 is for a source point inside the domain. For the BEM, the source point has to be moved on to the boundary. When the source point is on the boundary, a singularity occurs in the fundamental solution and Equation 21 has to be integrated in a special manner. In Figure 3, two boundaries are considered, Γ_ε for $r = \varepsilon$ at the source point and Γ_r which is equal to $\Gamma - \Gamma_\varepsilon$. In a two-dimensional case, these boundaries are lines, and for a

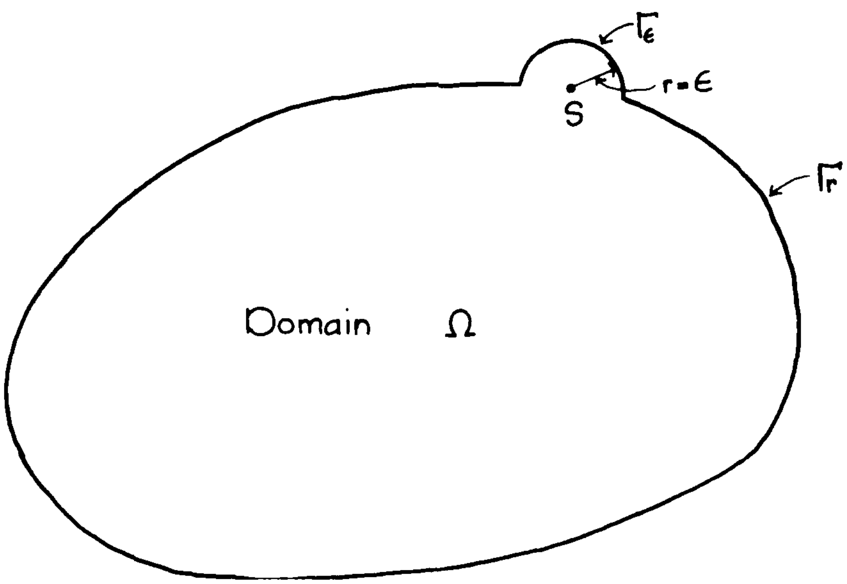

Figure 3. Augmented surface for integration on the boundary

three-dimensional case, they are surfaces. The integration has to be performed as $\varepsilon \to o$. For an explanation of the integration, let us consider

$$\int_{\Gamma} u_k t^*_{lk} \, d\Gamma = \int_{\Gamma_\varepsilon} u_k t^*_{lk} \, d\Gamma_\varepsilon + \int_{\Gamma_r} u_k t^*_{lk} \, d\Gamma_r \tag{22}$$

The first part of the integral in Equation 22 can be shown to be $-(u_k/2)$, after substitution of the fundamental traction into the integral sign and noting that $\varepsilon \equiv r$. It can also be shown that the second part does not introduce any new term when $\varepsilon \rightarrow o$, when Equation 21 is used on the boundary. Thus, the boundary integral equation on the boundary is written as

$$c_s u_l(s) + \int_{\Gamma} t^*_{lk} u_k \, d\Gamma = \int_{\Gamma} u^*_{lk} t_k \, d\Gamma \tag{23}$$

where $c_s = 1/2$ when boundary is smooth, and $c_s = 1$ if s is inside the domain. The value of c_s for higher order elements can be derived separately or calculated from rigid body motion criteria (Brebbia and Walker 1972; Brebbia, Telles, and Wrobel 1984).

Fundamental Solution

15. The fundamental solution is an analytical point-load solution in the domain and this is used to convert the domain integral into a boundary integral. The solution of Equation 19 is the fundamental solution of displacements and tractions for elastostatics problems. For three- and two-dimensional cases, Kelvin (Love 1927) developed the fundamental solution due to a point load in an infinite continuum. Several others (Brebbia and Walker 1972; Brebbia, Telles, and Wrobel 1984; and Hentenyi 1946) produced solutions for different domains and loads. The use of a particular fundamental solution is a matter of choice and each has its own advantages in application. Kelvin's solution is adopted in this work for two reasons: first, it can be used for bounded domains; second, it is convenient and required to solve problems in layered media. The expression for the fundamental solution of Kelvin for displacements and tractions for a unit load in an infinite continuum are given below:

$$u^*_{ij}(s,q) = \frac{1}{16\pi\,(1 - \nu)\,Gr} \left\{(3 - 4\nu)\delta_{ij} + r_{,i} r_{,j}\right\} \tag{24}$$

for three-dimensional, and

$$u^*_{ij}(s,q) = \frac{-1}{8\pi(1-\nu)G} \left\{(3 - 4\nu)\ \ln(r)\delta_{ij} - r_{,i}r_{,j}\right\} \tag{25}$$

for two-dimensional plane-strain problems. Corresponding traction functions are

$$t^*_{ij}(s,q) = \frac{-1}{4\alpha\pi(1-\nu)r\alpha} \left\{\left[(1 - 2\nu)\delta_{ij} + \beta r_{,i}r_{,j}\right]\frac{\partial r}{\partial n} - (1 - 2\nu)(r_{,i}n_j - r_{,j}n_i)\right\} \tag{26}$$

where $\alpha = 2\ ,\ 1\ ;\ \beta = 3\ ,\ 2$ for three- and two-dimensional plane strain, respectively. Also, $r = r(s,q)$ represents the distance between the load point s and the field point q and its derivatives are taken with reference to the coordinates of q, i.e.,

$$r = (r_i r_i)^{1/2} = |s - q|\ ,$$

$$r_i = x_i(q) - x_i(s)\ ,$$

$$r_{,i} = \frac{\partial r}{\partial x_i(q)} = \frac{r_i}{r}$$

Interpolation Functions and Numerical Analysis

16. An analytical intergration of the boundary-element equation as seen in Equation 23 is extremely tedious and not practical for solving engineering problems. These integrations are performed in a piecewise manner on the boundary using discrete boundary elements. The boundary is discretized into line elements in a two-dimensional problem and surface elements in a three-dimensional problem.

17. The variations of the unknown displacements and tractions on the boundary are achieved through the use of interpolation functions, namely,

$$\begin{aligned} u_i &= \phi_{ij}U^n_j \\ t_i &= \psi_{ij}T^n_j \end{aligned} \tag{27}$$

where U^n_j and T^n_j are the nodal values of displacement and traction vectors

on the n^{th} boundary element, respectively, and ϕ_{ij} and ψ_{ij} are the interpolation functions. The simplest of these is the constant element, where the displacements and tractions are considered to be constants within the elements. In the case of linear elements, the displacements and tractions vary linearly within the element. Higher order elements can also be formulated (Banerjee and Butterfield 1981; Brebbia, Telles, and Wrobel 1984).

18. The boundary is discretized into a number of constant elements. Then Equation 23 is applied on the boundary in a discrete form. The corresponding boundary-element equation in the constant elements would be of the form,

$$c(s)u_i(s) + \sum_{j=1}^{M} \left\{ \int_{\Gamma_j} t^*_{ij} \, d\Gamma \right\} U_j = \sum_{j=1}^{M} \left\{ \int_{\Gamma_j} u^*_{ij} \, d\Gamma \right\} T_j \tag{28}$$

where

M = total number of boundary elements

Γ_m = m^{th} boundary element

U_j and T_j = displacements and tractions in the element j

Equation 28 relates the i^{th} node integration (source point s) and the integration is carried out throughout the boundary on the M elements. This is done sequentially by numerical integration, using Gauss quadrature formulas. The source point on each element is chosen to be the midpoint of the element. Hence, Equation 28 is applied at every element at its midpoint to form the system equations. The integrals over each element now become 2×2 matrices and are represented as $\hat{H}_{ij}$ and G_{ij}. Hence, Equation 28 becomes

$$c_i(s)U_i(s) + \sum_{j=1}^{M} \hat{H}_{ij}U_j = \sum_{j=1}^{M} G_{ij}T_j \tag{29}$$

Equation 29 relates the value of displacements U at the midpoint of the element i, namely the source point with the displacements and tractions at all the elements on the boundary, including the source point. Equation 29 can be written as,

$$\sum_{j=1}^{M} H_{ij}U_j = \sum_{j=1}^{M} G_{ij}T_j \tag{30}$$

where

$$H_{ij} = \hat{H}_{ij} \quad \text{for} \quad i \neq j$$

$$H_{ij} = \hat{H}_{ij} + c_i \quad \text{for} \quad i = j$$

When $i = j$, in Equation 29, the integration becomes singular and has to be evaluated analytically or by other means. It is easier to calculate H_{ii} using rigid body considerations and for constant element it works out to be 0.5 (Brebbia and Walker 1972). G_{ii} can be calculated analytically or by a logarithmically weighted numerical integration formula.

19. The system equations now can be written as

$$[H]\{U\} = [G]\{T\} \tag{31}$$

with known displacements and tractions, specified as boundary conditions. $[H]$ and $[G]$ are square matrices of the order $2 \times M$.

Solution of System Equations

20. Whenever displacements are prescribed, the tractions cannot be prescribed, and vice versa. Knowing the known displacements and tractions, and rearranging the set of equations with unknowns on the left-hand side and knowns at the right-hand side, the entire Equation 31 is rearranged as a set of linear simultaneous equations.

$$[A]\{x\} = \{b\} \tag{32}$$

Solving Equation 32, we get all the unknown displacements and tractions on the boundary.

PART III: COUPLING OF BOUNDARY- AND FINITE-ELEMENT METHODS

Introduction

21. The BEM has been found to be a very powerful technique for solving stresses and deformations of large continuum where the boundaries are at large distances. This method is used to represent large soil media in the soil-structure interaction problems. The FEM is used to represent the structure; properties such as complex geometry, heterogeneity, nonlinearity, reinforcement, etc., are better modeled by the FEM. For an elastic continuum, the BEM yields better results with relatively lesser number of unknowns with easy preparation of input data. If one needs to use nonlinear properties of the soil in the immediate vicinity of the structure, it is recommended at present to use the FEM for the nonlinear portion of the soil media. The use of these two methods make the analysis computationally and economically more efficient.

Equations Used in Coupling

22. There are two basic procedures for combining the two methods (Brebbia and Walker 1972; Brebbia, Telles, and Wrobel 1984). One is to convert the finite-element equations to suit the boundary-element equations. This has been the main technique used by many researchers. However, this procedure has serious efficiency problems, especially when the FEM has nonlinear behavior. The method adopted here is in the reverse order; i.e., the boundary-element equation is transformed into an equivalent-stiffness matrix and added to the finite-element half-banded stiffness-matrix equation. This technique has many advantages in solving soil-structure interaction problems.

23. Consider two regions, Ω_1 and Ω_2, with different material properties and geometries as shown in Figure 4. Region Ω_1 is divided into finite elements and region Ω_2 into boundary elements. Coupling the two models is done by using equilibrium and compatibility on the interface g_B :

- a. Equilibrium of tractions; i.e., the tractions on g_B interface for region Ω_1 and Ω_2 should be equal and opposite.

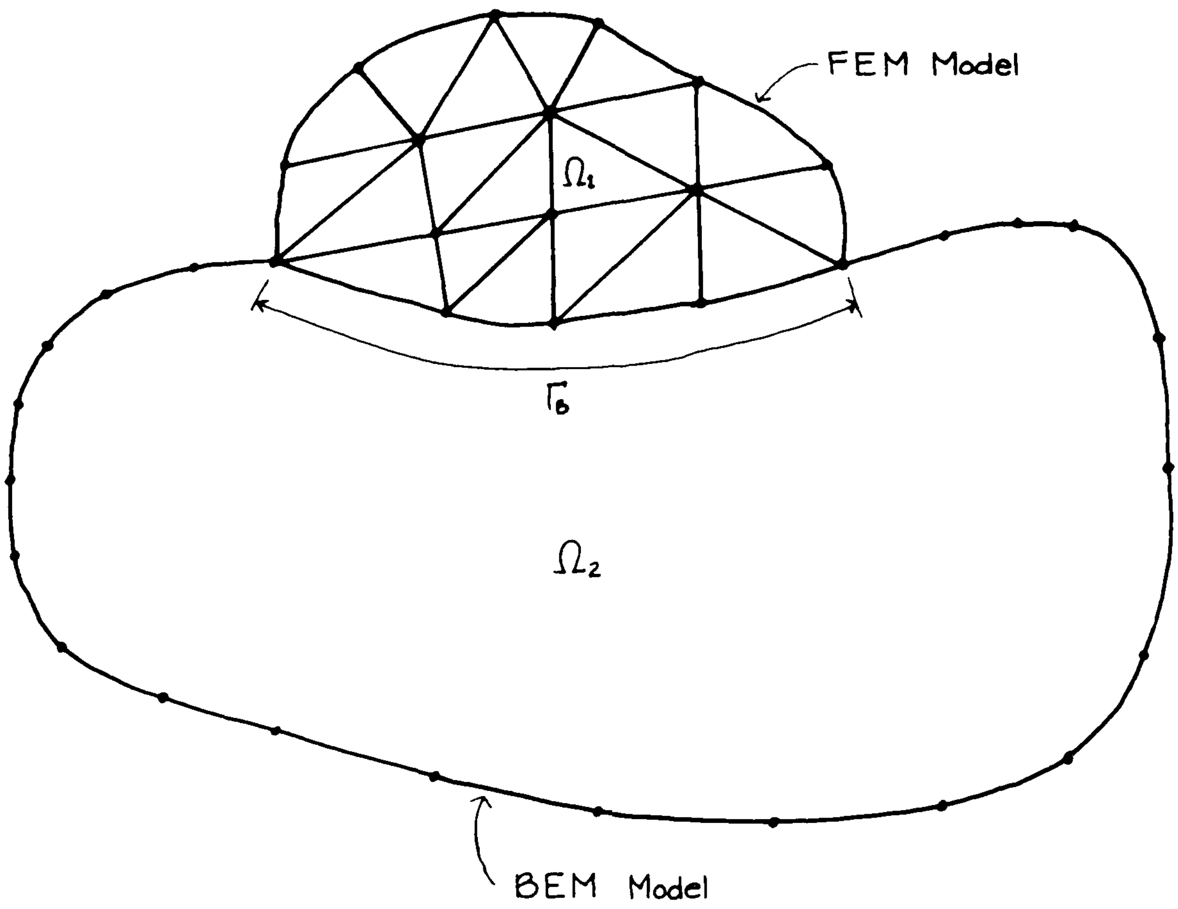

Figure 4. Domain with different properties

b. Compatibility of displacements; i.e., displacements on g_B interface for region Ω_1 and Ω_2 should be equal.

Finite-Element Equation

24. The structure is discretized into plane-strain finite elements in our analysis. The structure stiffness matrix is developed using the computer code, and this includes the soil-structure interface, denoted by g_B in Figure 4. The finite-element stiffness-matrix equation will be

$$\begin{bmatrix} K_{SS} & K_{SB} \\ K_{BS} & K_{BB} \end{bmatrix} \begin{Bmatrix} U_S \\ U_B \end{Bmatrix} = \begin{Bmatrix} F_S \\ F_B \end{Bmatrix} \tag{33}$$

where

K_{SS} = soil stiffness

K_{SB}, K_{BS} = off-diagonal stiffness beams

K_{BB} = beam stiffness

U_S = soil displacements

U_B = beam displacements

F_S = forces on soil

F_B = forces in beam

where the square matrix is the global-stiffness matrix of the finite-element portion, U_B and F_B are the displacement and force vectors of the boundary-element interface and U_S and F_S are the remaining displacement and force vectors of the finite-element system. The finite-element stiffness matrix shown in Equation 33 is developed as a half-banded matrix for computational economy.

Boundary-Element Equation

25. Using the BEM, a stiffness matrix representing the soil media has to be developed on the interface. This should be in such a form that it is compatible with the finite-element system. Therefore, the boundary-element stiffness-matrix equation should be of the type:

$$[k_B]\{U_B\} = -\{F_B\} + \{f_B\} \tag{34}$$

where f_B is a condensed force vector representing the prescribed forces and displacements on the boundary of the soil medium. The development of the condensed equation (Equation 34) representing the soil medium for a hydraulic U-lock structure is discussed in the following section.

Soil Stiffness

26. To obtain a condensed stiffness matrix $[k_B]$ to represent soil, Kelvin's fundamental solution as shown in Equations 24 through 26 is used for the formulation of the boundary-element equations. Figure 5 shows the BEM for a U-lock structure. Advantage in symmetry of the problem is taken care of in the computer code.

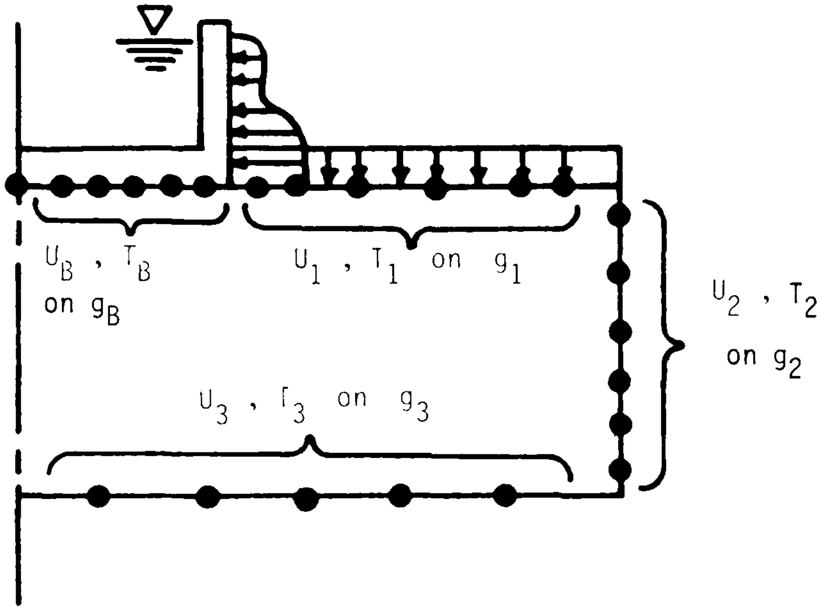

Figure 5. Boundary-element model for a U-lock structure

27. The boundary-element equations are developed using Equation 26 and the final set of matrices will be of the form:

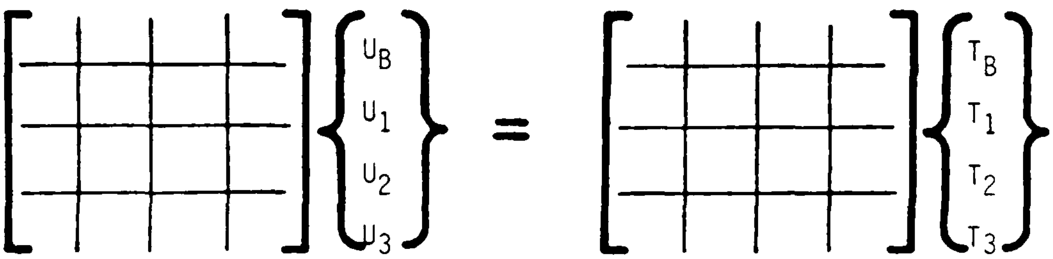

H-Matrix **G-Matrix**

where U and T are the nodal displacement and traction vectors on the four boundaries g_B , g_1 , g_2 , and g_3 as shown in Figure 5. The subscripts on U and T denote the respective boundaries. The following boundary conditions are prescribed for the problem:

on g_1 , $T_{1x} = 0$,
$T_{1y} = h$, a prescribed traction;
on g_2 , $U_{2x} = 0$,
$T_{2y} = 0$;
on g_3 , $U_{3y} = 0$,
$T_{3x} = 0$; and
on g_B , both U_B and T_B are unknowns.

Considering the prescribed and the unknown components of displacements and tractions, the H and G matrices can be reorganized such that the new H and G matrices are:

$$\begin{bmatrix} H_{11} & H_{12} \\ H_{21} & H_{22} \end{bmatrix} \begin{Bmatrix} U_B \\ V_U \end{Bmatrix} = \begin{bmatrix} G_{11} & G_{12} \\ G_{21} & G_{22} \end{bmatrix} \begin{Bmatrix} T_B \\ V_P \end{Bmatrix} \tag{35}$$

where V_P and V_U are vectors representing the prescribed and the unknown components of all displacements and tractions on g_1 , g_2 , and g_3 . The sizes of submatrices of H and G correspond to the orders of the interface vectors U_B and V_U , respectively. From Equation 35

$$V_U = H_{22}^{-1}(G_{21}T_B + G_{22}V_P - H_{21}U_B \tag{36}$$

and substituting this into part of Equation 35,

$$(H_{11} - H_{12}H_{22}^{-1}H_{21})U_B = (G_{11} - H_{12}H_{22}^{-1}G_{21})T_B + (G_{12} - H_{12}H_{22}^{-1}G_{22})V_P \tag{37}$$

this equation can be reduced to

$$[k_B]\{U_B\} = -\{F_B\} + \{f_B\} \tag{38}$$

where k_B is the required stiffness matrix of the soil medium, F_B is the equivalent nodal forces of the traction vector T_B , and f_B is an equivalent force vector representing the prescribed forces and displacements on g_1 , g_2 , and g_3 . The development k_B and f_B appears to be quite cumbersome. But, the computations can be simplified considerably by using a static condensation procedure (Vesic 1961). Using the Gauss/Jordan elimination procedure, if one transforms both H and G matrices such that H_{22} is made into an identity matrix and H_{12} to a null matrix, then the new transformed matrices H^*_{11} , G^*_{11} , and G^*_{12} are, i.e.,

$$H^*_{11}U_B = G^*_{11}T_B + G^*_{12}V_P \tag{39}$$

the matrices within the respective brackets in Equation 36. Again using

elimination procedure, Equation 39 is transformed such that G^{*}_{11} is made into an identity matrix, i.e.,

$$H^{*}_{11}U_B = T_B + G^{**}_{12}V_P \tag{40}$$

Transforming nodal tractions vector T_B to equivalent nodal force vector $-F_B$ in Equation 40 and adding this to Equation 33, we get the desired Equation 42. This is achieved by multiplying both sides of Equation 40 by a distribution matrix M, to convert tractions into nodal forces. Thus, we have

$$[MH^{**}_{11}]U_B = MT_B + MG^{**}_{12}V_P = -\{F_B\} + \{f_B\} \tag{41}$$

i.e.,

$$[k_B]\{U_B\} = -\{F_B\} + \{f_B\} \tag{34 bis}$$

Coupling of Finite-Element and Boundary-Element Matrices

28. Having developed the stiffness matrices of the structure and the soil as shown in Equations 33 and 34, the coupling is done ensuring compatibility and equilibrium at the interface. Now the combined FEM/BEM model can be written as

$$\begin{bmatrix} K_{SS} & K_{SB} \\ K_{BS} & K_{BB} + k_B \end{bmatrix} \begin{Bmatrix} U_S \\ U_B \end{Bmatrix} = \begin{Bmatrix} F_S \\ f_B \end{Bmatrix} \tag{42}$$

This equation is readily solved to get the displacements and stresses of the structure.

Asymmetry of Boundary-Element Stiffness Matrix

29. The stiffness matrix $[k_B]$ formed from the boundary-element domain is generally asymmetric. This poses problems for addition into the symmetric-stiffness matrix of the finite-element region. The asymmetry of the boundary element is not new and has been reported in literature before (Banerjee and Butterfield 1981; Brebbia, Telles, and Wrobel 1984; Georgiou 1981; Hartmann 1981). This has been attributed to three factors; namely, discretization of

the boundary-element domain, collocation process, and the nature of the fundamental solution. To alleviate this anomaly, the boundary-element stiffness matrix is symmetrized, discarding the unsymmetric part. This has been justified by Georgiou (1981) by showing examples, the results of which are reasonably accurate. A detailed mathematical procedure to derive a symmetric stiffness matrix is explained by Hartmann (1981) in that by solving $G^{-1}Hu = t$ with Galerkin's method or by minimizing a potential $\phi(u)$, a symmetric stiffness matrix is guaranteed.

30. In this present work, the boundary-element stiffness matrix is symmetrized by averaging the off-diagonal terms, by the principle of least squares as suggested by Brebbia and Walker (1972). It is found that the error involved is very small and negligible that

$$\frac{k_{ij} - k_{ji}}{k_{ii}} \leq 0.002\%$$

Compatible Boundary Stiffness Matrix

31. The boundary elements representing the soil are assumed to have a constant variation of displacements and traction over their length. Thus, on the interface the boundary elements will lie in between the finite-element nodes. The condensed effective stiffness of the soil portion obtained by Equation 34 has to be made compatible with the finite-element stiffness matrix representing the structure for coupling.

Coupling of stiffness affected

32. The coupling of stiffness from the constant boundary-element formulation of the soil to the finite-element stiffness of the structure is affected in two ways, as explained below.

- a. Method I. In this method, the midpoints of the boundary elements are positioned in such a way that they lie on the finite-element nodes of the structure at the interface. The stiffness at the ends of the boundary elements at the interface are reduced by half so as to correspond to the stiffness of the subgrade at the interface, to be added appropriately at the interface.
- b. Method II. In this method, the end points of the boundary elements coincide with the finite-element nodes. Therefore, the stiffness matrix of the subgrade from the boundary-element region will be lesser by two rows and two columns due to a node

lesser in boundary-element formulation. The condensed stiffness matrix at the interface, representing the subgrade, is expanded by premultiplying it by a transformation matrix and then postmultiplying it by its transpose. This transformation is possible by the use of contragradient law (Vallabhan and Jain 1972) and satisfies energy principles. Let U^b and F^b be the nodal displacements and forces at the midpoints of the boundary elements at the interface. Let U^f and F^f be the displacements and forces at the finite-element nodes at the interface. Let [T] be the transformation matrix which converts the finite-element displacements of the interface nodes into the boundary-element displacement at the midpoints. Therefore,

$$\{u^b\} = [T]\{u^f\} \tag{43}$$

By contragradient law,

$$\{F^f\} = [T]^t \{F^b\} \tag{44}$$

Transposing Equation 46 and postmultiplying by $\{u^f\}$,

$$\{F^f\}^t\{u^f\} = \{F^b\}^t[T]\{u^f\} = \{F^b\}^t\{u^b\} \tag{45}$$

i.e., the work done by the forces on the displacements of the finite-element systems is equal to the work done by the forces on the displacements of the boundary-element system.

Subgrade matrix

33. The condensed stiffness matrix of the subgrade is

$$\begin{aligned}
&[k_B]\{U_B\} = f_B \\
&[k_B][T][U_F] = \{F_B\} \\
&[T^T][k_B][T]\{U_F\} = [T^T]\{F_B\} = \{F_F\} \\
&[k_B]\{U_f\} = \{F_F\}
\end{aligned} \tag{46}$$

This method is more convenient and yields a better solution than Method I.

PART IV: SOIL-STRUCTURE INTERACTION PROBLEMS

A Typical Problem

34. Many researchers have validated the use of the BEM for solving stresses and displacements in linear continuum (Banerjee and Butterfield 1981; Brebbia and Walker 1972; and Brebbia, Telles, and Wrobel 1984) and hence, examples are not shown here for demonstrating the capabilities of the boundary-element method. On the other hand, examples are shown here to illustrate the coupling of the BEM and FEM for solving soil-structure interaction problems. A typical problem which concerns a hydraulic U-lock structure was selected for this purpose. This particular problem has been studied and solved by fellow researcher, Wilson (1974), who used other methods of analyses. The problem deals with a strip of plate of unit width resting on finite-soil media and is considered as one of place-strain type. The strip is modeled as a beam of length, L equal to 100 ft.* Two cases of depth d of beam are considered, one for depth equal to 5 ft and the other equal to 10 ft. Two values of the depth of the soil, H , were used; in the first case, H is set equal to 100 ft, and in the second case, H is set as 200 ft. The modulus of elasticity of the concrete beam E_b is taken as 3×10^6 psi . The modulus of elasticity of the soil E_s is varied such that the two values of the modular ratio $n = E_b/E_s$ are taken as 10 and 100, respectively. For convenience, in this analysis the Poisson's ratio of the concrete and the soil is set equal to 0.2, even though this is not a limitation of the methodology at all. Altogether, there are eight cases of beam/soil geometry and material properties for each loading case. Table 1 indicates the nomenclature for these eight cases. The load cases used here are:

a. A uniformly distributed load of 5 k/ft on top of the beam.

b. A concentrated load of 250 k at each end of the beam.

c. A concentrated moment of 5,000 ft-k at each end of the beam.

It is further assumed that the soil is resting on a smooth, [illegible] rock surface. The effect of the smoothness of the bottom boundary on the accuracy of the results is found to be negligible for the above geometry. Since we are

---

* A table of factors for converting non-SI units of measurement to SI (metric) units is presented on page 3.

dealing with finite dimensions of soil media, it is assumed that the vertical boundaries at a distance of 200 ft away from the center line are considered smooth. All these boundary conditions are selected only from a practical design point of view, and they reflect no limitations of the technique. The loads, geometry, and the boundary conditions of the problem are illustrated in Figure 6. Thus far, we have 24 problems to be solved.

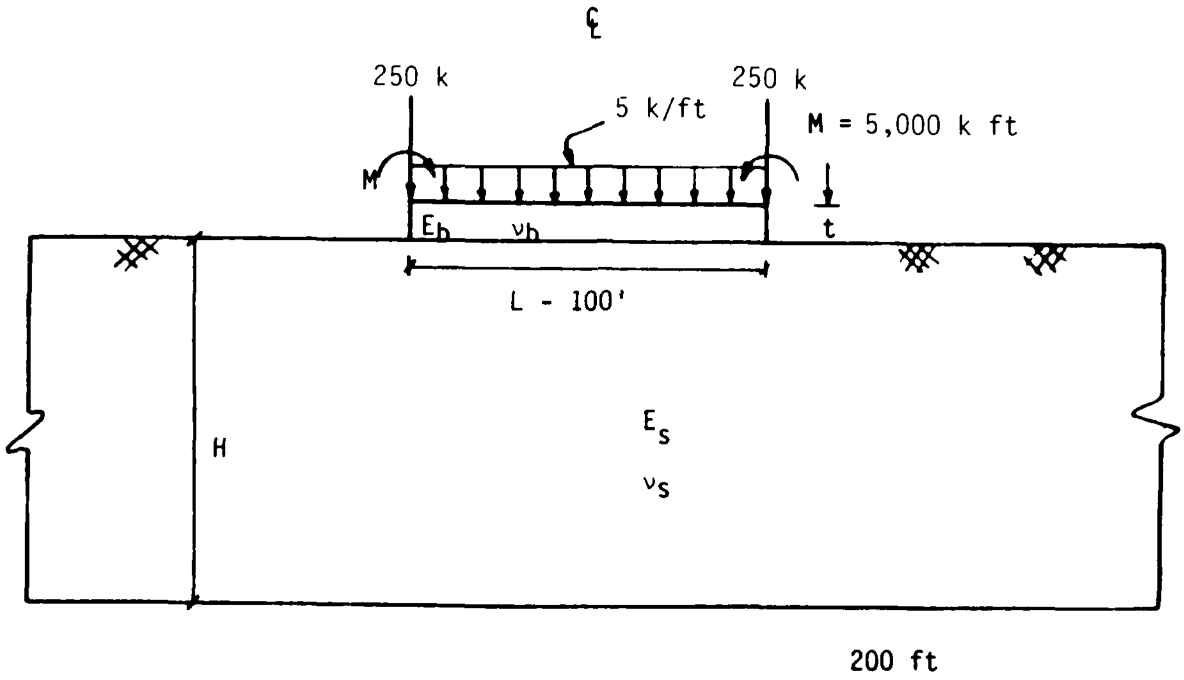

E_b = 3,000 ksi

$\nu_b = \nu_s = 0.2$

H = 100 ft, 200 ft

Bottom and sides are smooth boundaries

L = 100 ft

L/t = 10, 20

$n = \frac{E_b}{E_s}$ = 10, 100

Figure 6. Details of the example problem

35. Another question which comes into the analysis is the compatibility of horizontal displacements between the structure and the soil at the interface. It is a common practice in beam-on-elastic-foundation studies to ignore the compatibility of horizontal displacements at the interface. If one ignores this condition, we are essentially assuming that the soil interface is perfectly smooth. Thus, the analysis is performed in two categories. In the first category, the compatibility of horizontal displacements are neglected, thereby making the soil as a smooth boundary. In the second case, compatibility of horizontal displacements on the interface are enforced.

Discretization of the Example Problem

36. Due to the symmetry of the problem only half the domain was used for discretizations. Rectangular finite elements with 8 deg of freedom are employed here. The beam is discretized into five layers with ten elements in each layer. This discretization is found to model the accurate bending of beams for displacements and stresses. The boundary-element discretization must be made compatible with the finite-element discretization at the interface. The sizes of the boundary elements are varied such that wherever the displacements and stresses are small or uniform, larger elements are used as shown in Figure 7. A convergence study was made on the number of boundary elements in the combined model, and it was found that the discretization with 40 elements shown in Figure 7 gave essentially the same results with larger numbers of boundary elements.

37. In order to verify the accuracy of the finite-element/boundary-element model, a complete finite-element study is also made for four selected cases, such as 5, 6, 7, and 8 for each loading condition. The finite-element discretization for the problem in the loadings and boundary conditions are shown in Figure 8.

Presentation of Results

38. The results for various cases are presented in graphical and tabular form. They relate principally to the vertical displacements and tractions at the interface.

39. These results are seen in a clearer perspective in graphical form. Parts a of Figures 9 through 20 show the plots of vertical displacement at the interface for each loading condition. Parts b of Figures 9 through 20 show the plots of corresponding vertical tractions at the interface. These graphs are analyzed for the first category, i.e., where the compatibility of horizontal displacements are not enforced at the interface.

40. In all tables, the displacements shown at nodes 1 to 11 are from the line of symmetry at 5-ft intervals, at the soil-structure interface. In the case of vertical traction at the soil-structure face, the values are a constant in each of the boundary elements and are shown at the midpoint of each boundary element. Tables A-1, A-3, and A-5 display the vertical

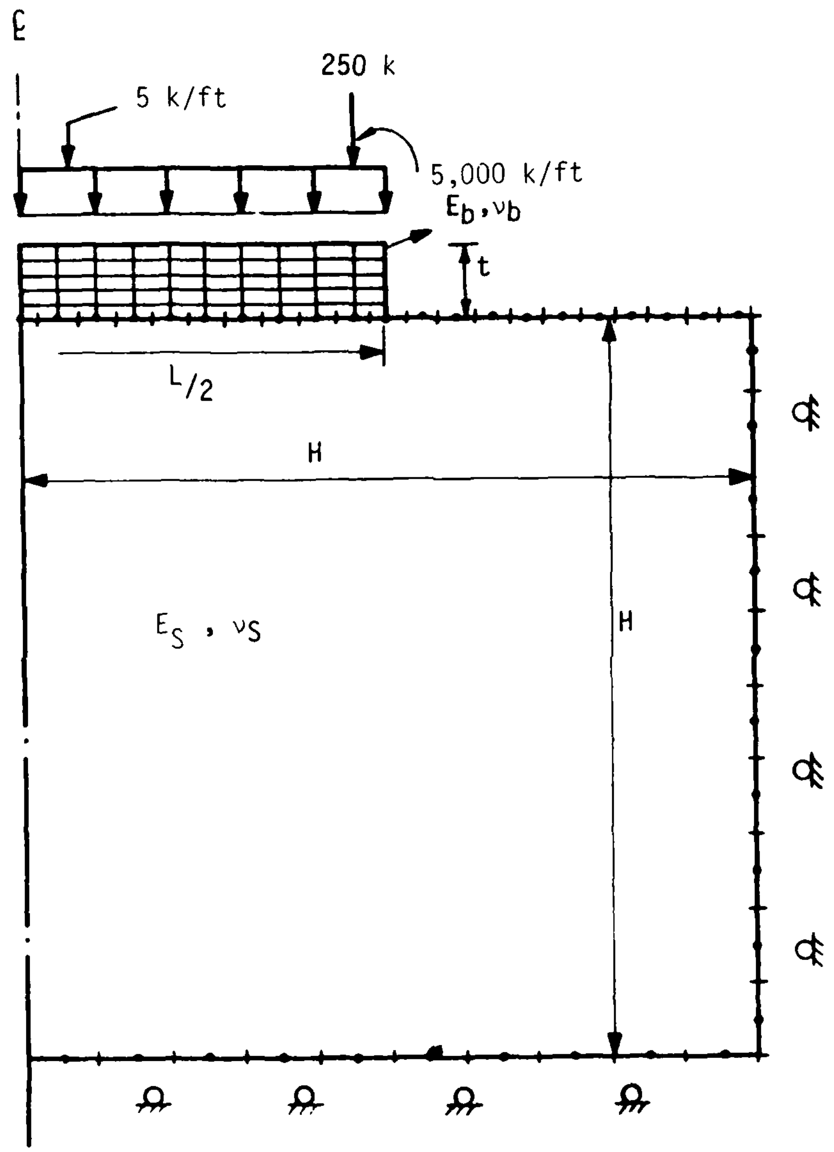

Figure 7. Discretization of the combined model

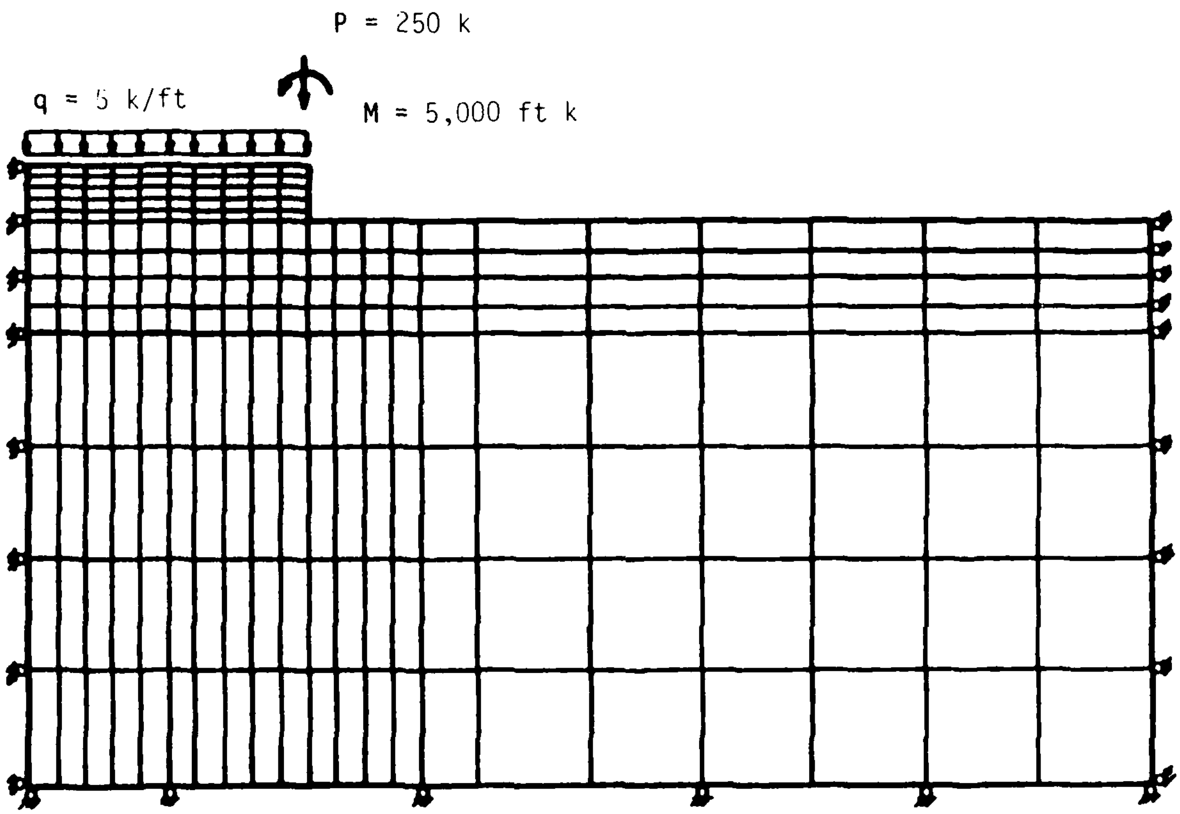

Figure 8. Discretization of the finite-element mesh

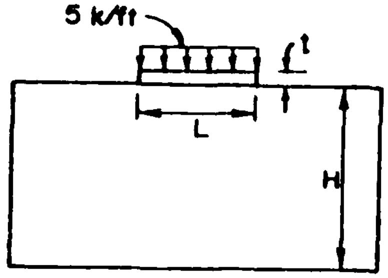

	H/L	L/t	$n = E_b/E_s$
Case 1	1	10	10
Case 2	1	10	100

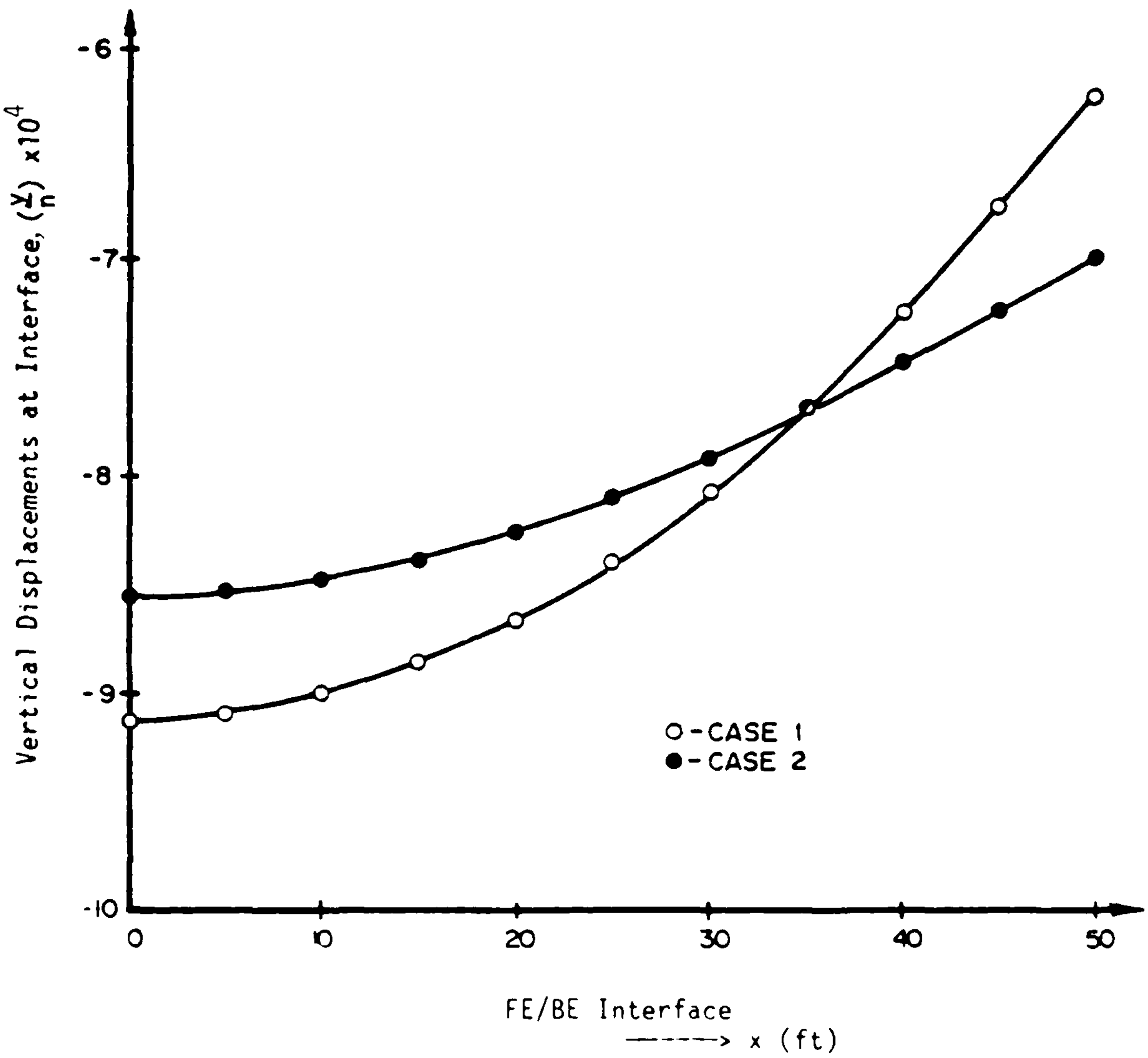

Figure 9a. Vertical displacements at the interface for cases 1 and 2 with uniformly distributed load 5 k/ft on top of beam

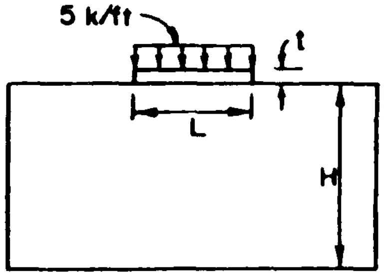

	H/L	L/t	$n = E_b/E_s$
Case 1	1	10	10
Case 2	1	10	100

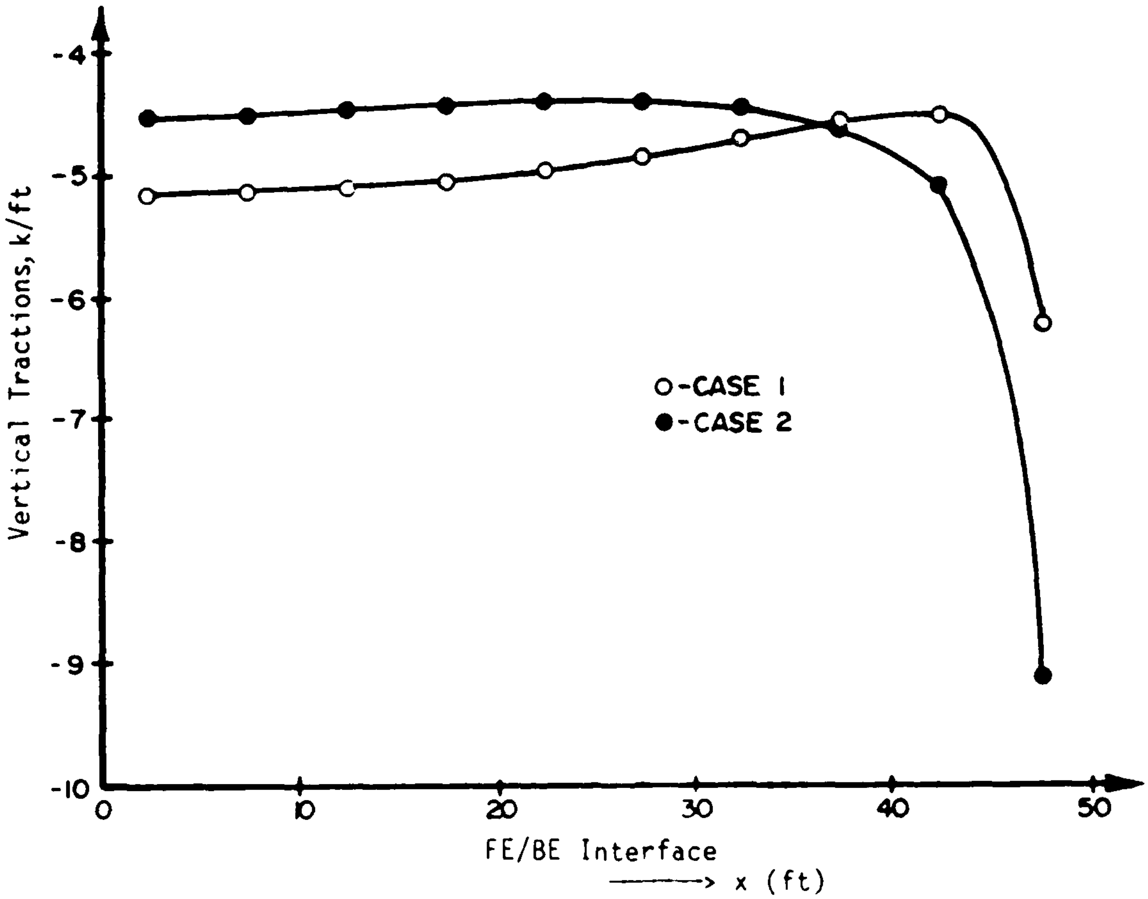

Figure 9b. Vertical tractions at the interface for cases 1 and 2 with uniformly distributed load 5 k/ft on top of beam

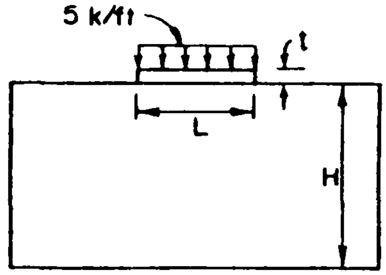

	H/L	L/t	$n = E_b/E_s$
Case 3	1	20	10
Case 4	1	20	100

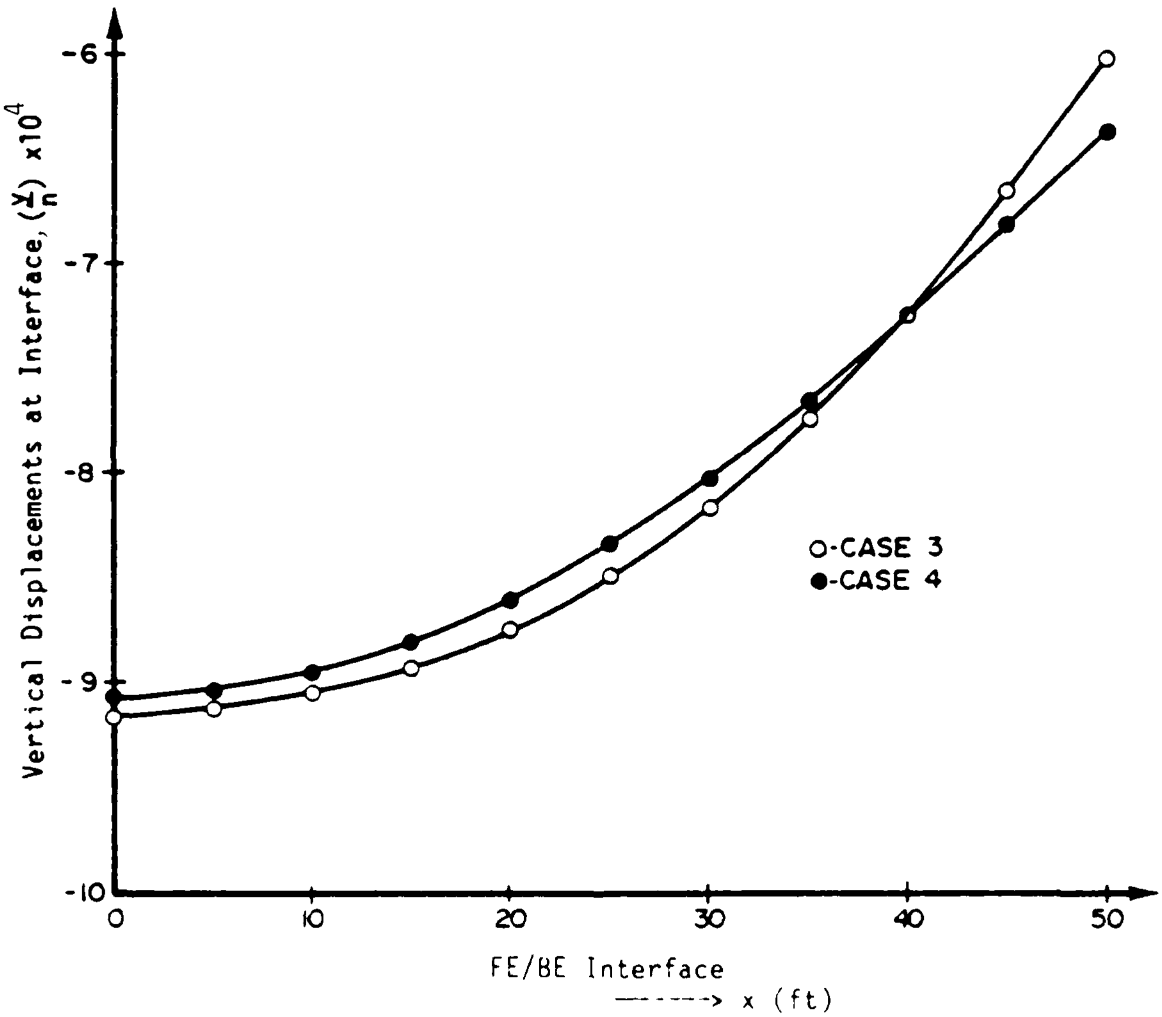

Figure 10a. Vertical displacements at the interface for cases 3 and 4 with uniformly distributed load 5 k/ft on top of beam

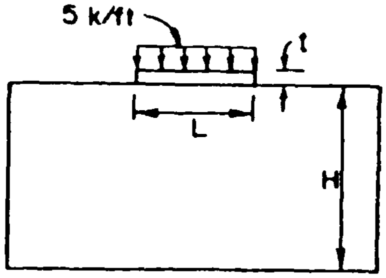

	H/L	L/t	$n = E_b/E_s$
Case 3	1	20	10
Case 4	1	20	100

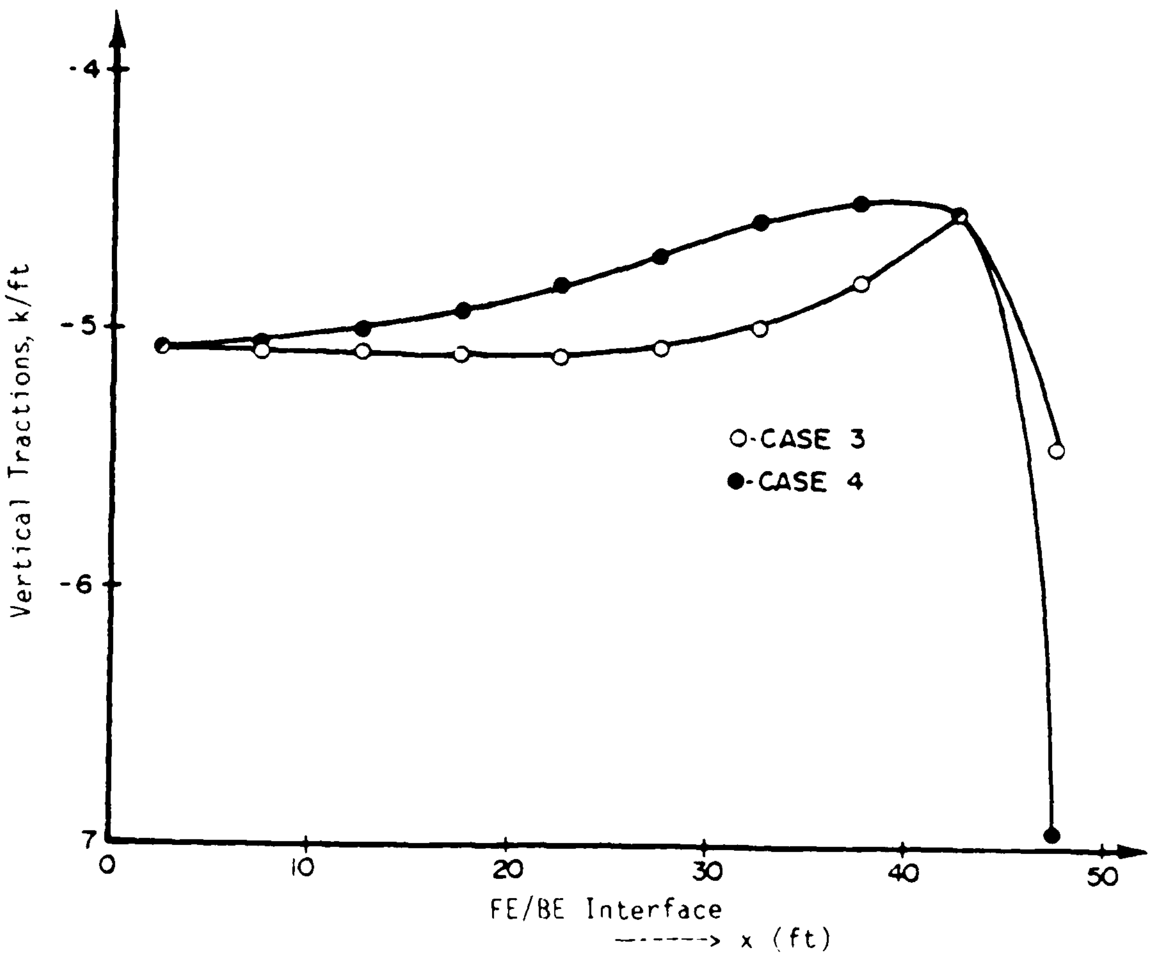

Figure 10b. Vertical tractions at the interface for cases 3 and 4 with uniformly distributed load 5 k/ft on top of beam

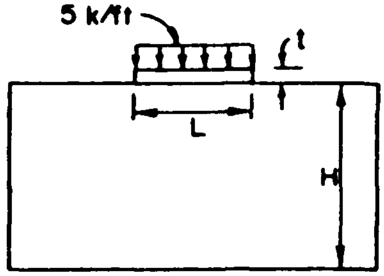

	H/L	L/t	$n = E_b/E_s$
Case 5	2	10	10
Case 6	2	10	100

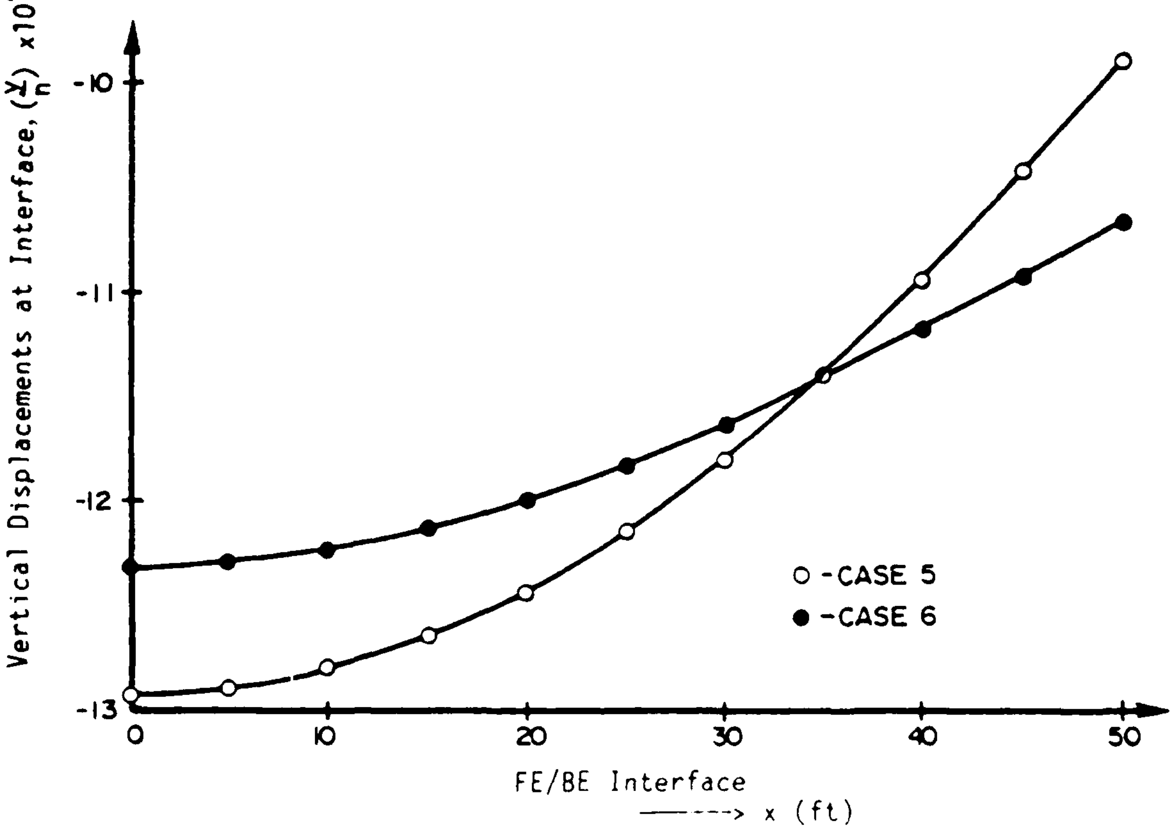

Figure 11a. Vertical displacements at the interface for cases 5 and 6 with uniformly distributed load 5 k/ft on top of beam

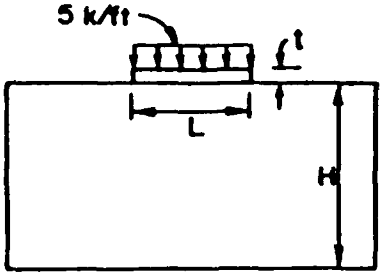

	H/L	L/t	$n = E_b/E_s$
Case 5	2	10	10
Case 6	2	10	100

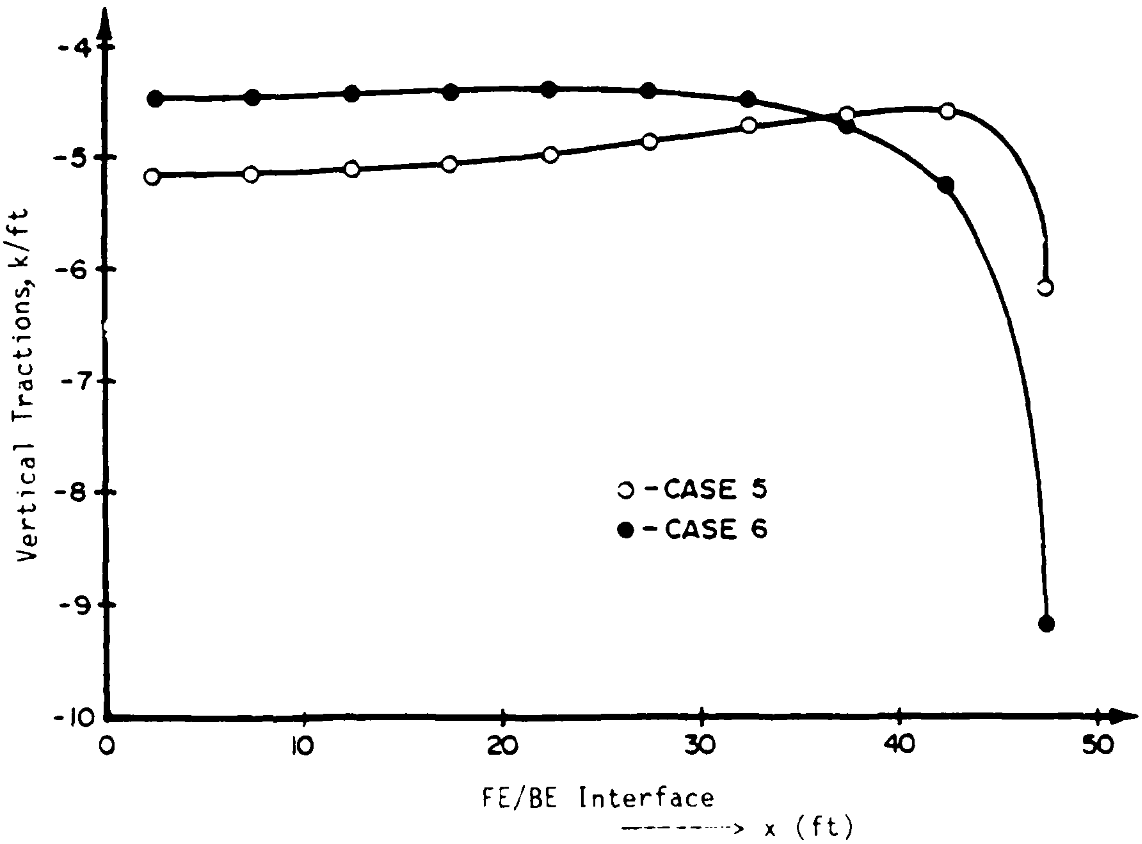

Figure 11b. Vertical tractions at the interface for cases 5 and 6 with uniformly distributed load 5 k/ft on top of beam

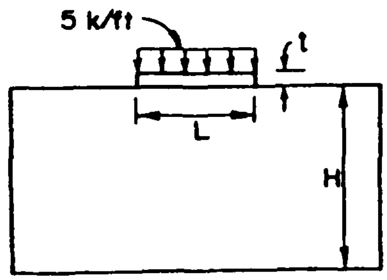

	H/L	L/t	$n = E_b/E_s$
Case 7	2	20	10
Case 8	2	20	100

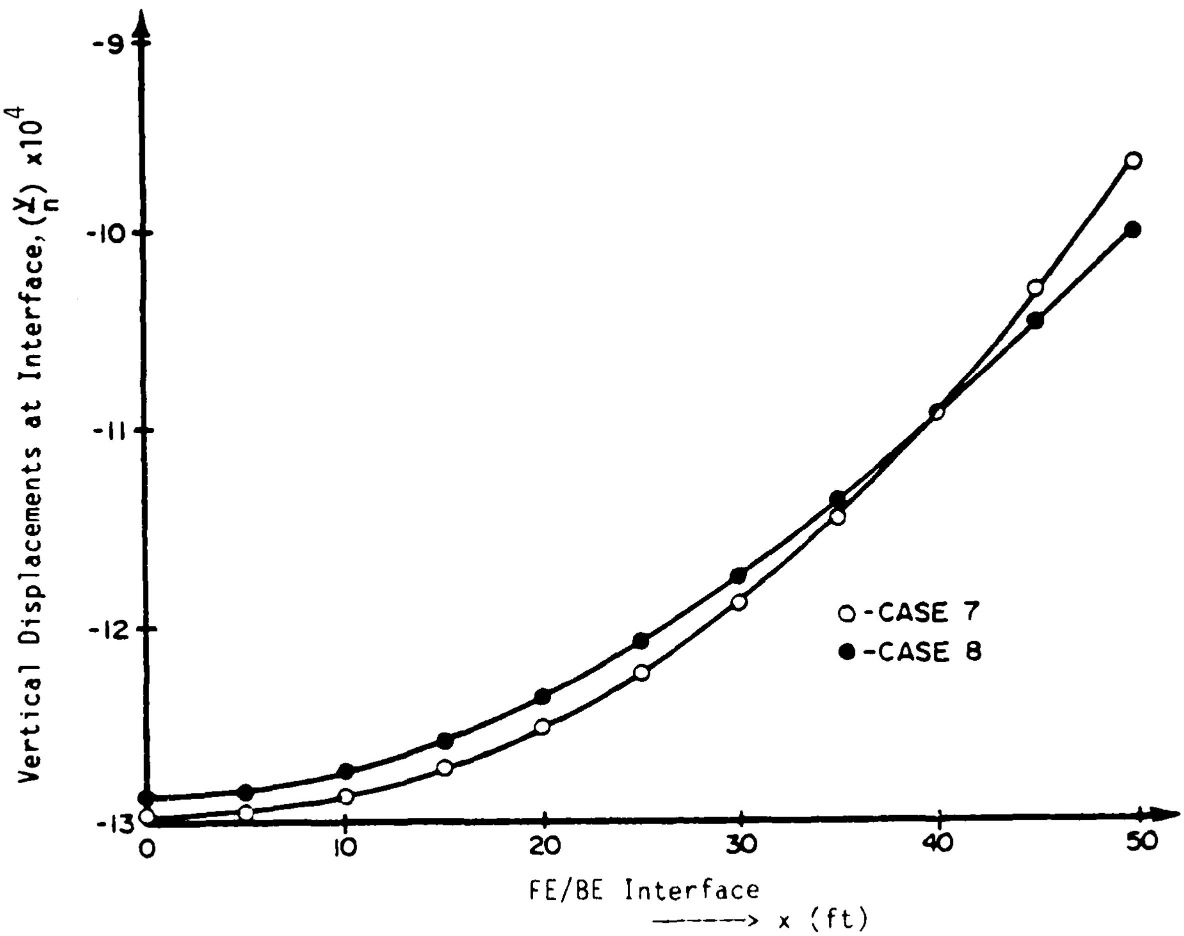

Figure 12a. Vertical displacements at the interface for cases 7 and 8 with uniformly distributed load 5 k/ft on top of beam

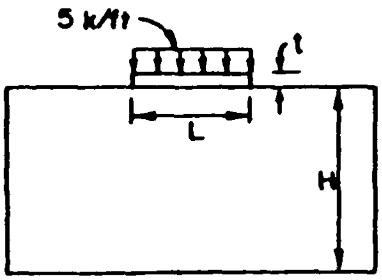

	H/L	L/t	n = E_b/E_s
Case 7	2	20	10
Case 8	2	20	100

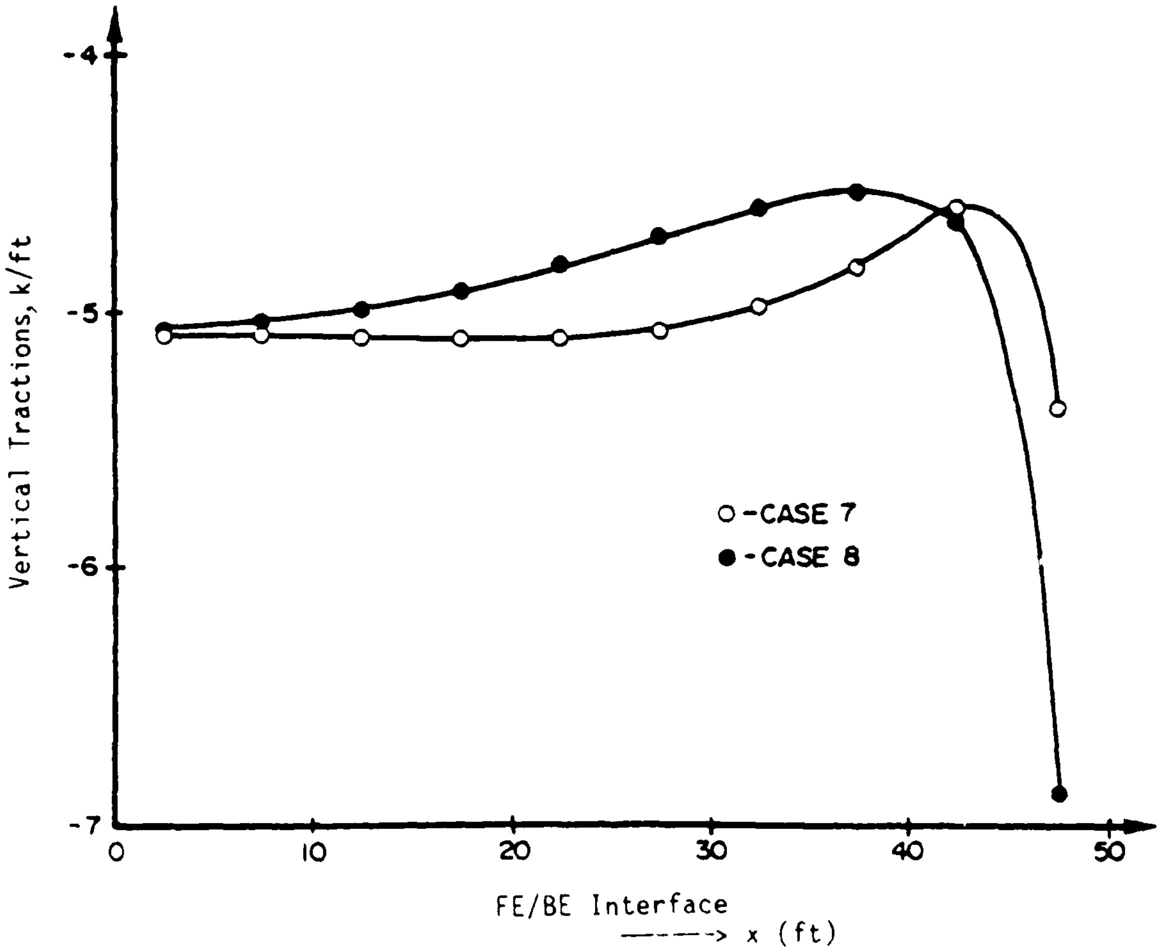

Figure 12b. Vertical tractions at the interface for cases 7 and 8 with uniformly distributed load 5 k/ft on top of beam

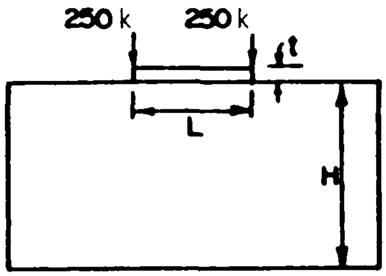

	H/L	L/t	$n = E_b/E_s$
Case 1	1	10	10
Case 2	1	10	100

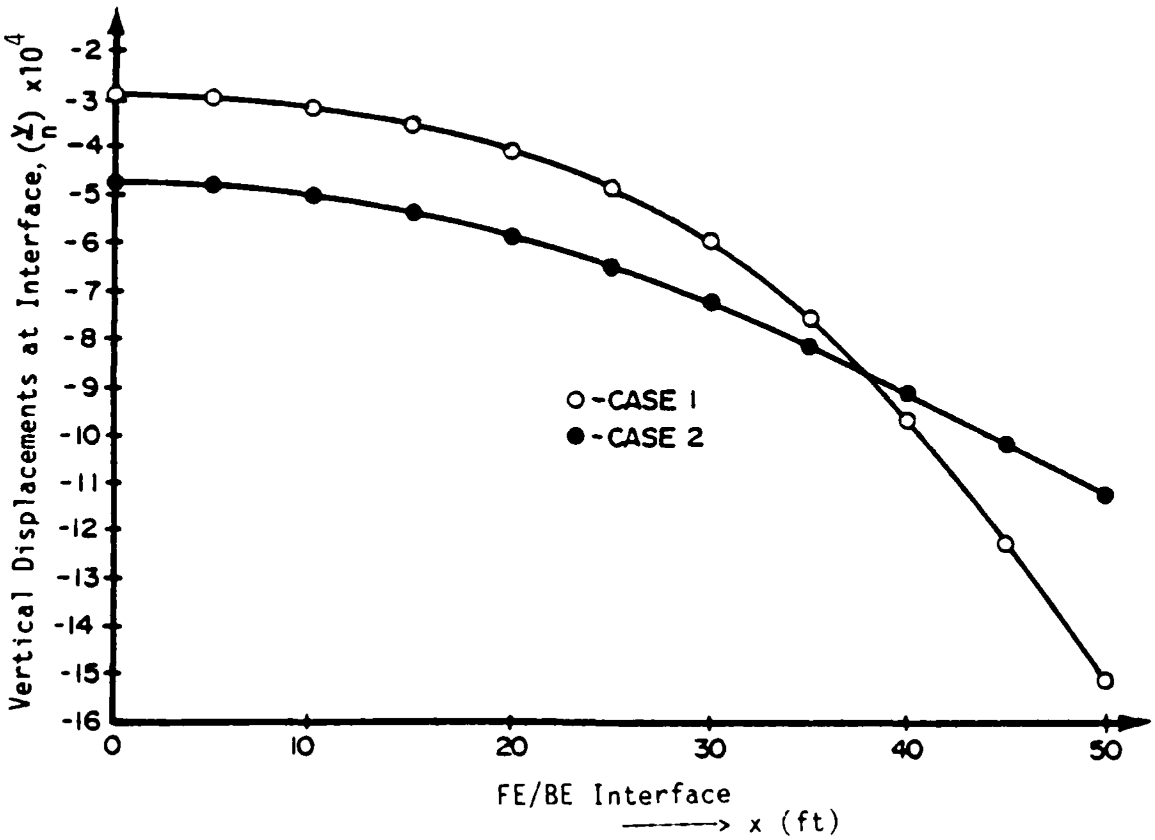

Figure 13a. Vertical displacements at the interface for cases 1 and 2 with concentrated load of 250 k at each end of the beam

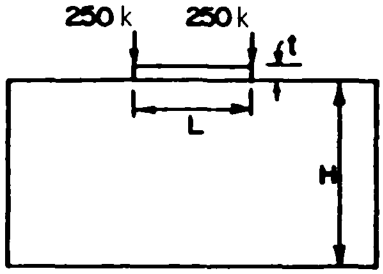

	H/L	L/t	$n = E_b/E_s$
Case 1	1	10	10
Case 2	1	10	100

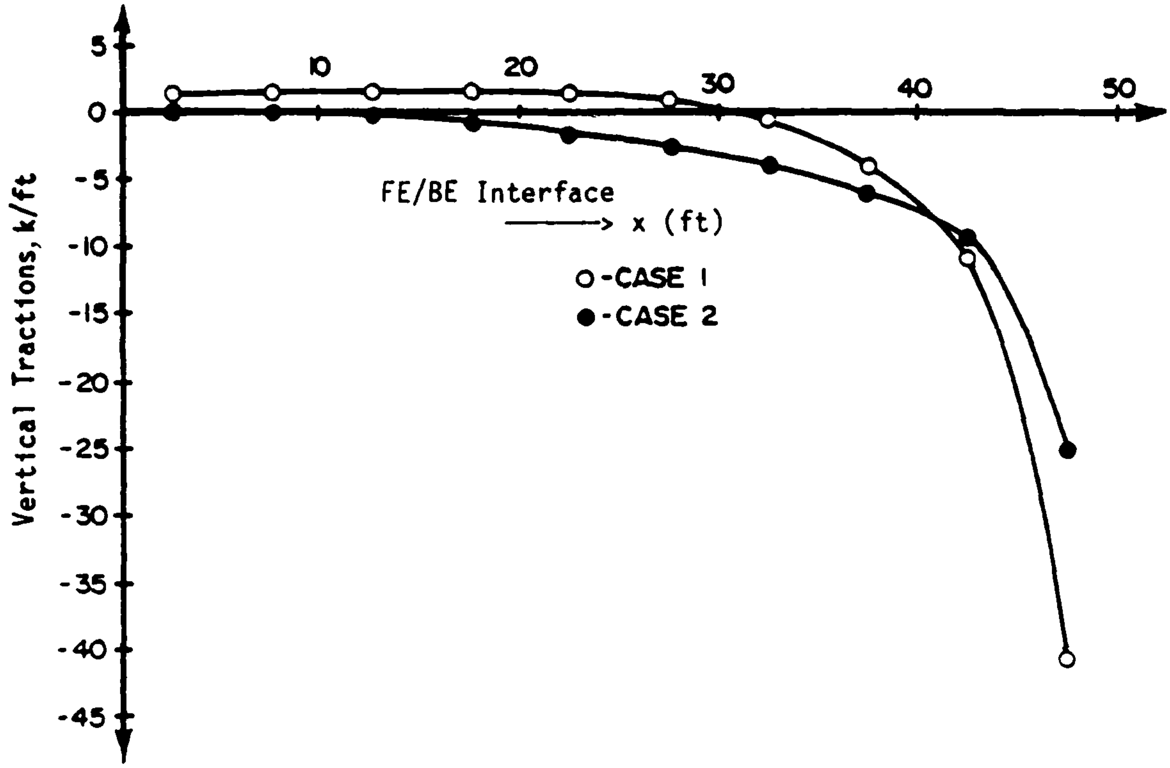

Figure 13b. Vertical tractions at the interface for cases 1 and 2 with concentrated load of 250 k at each end of the beam

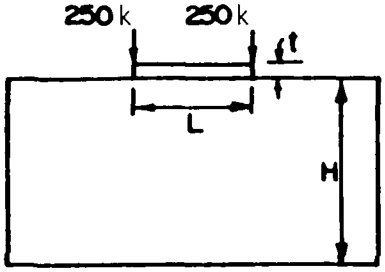

	H/L	L/t	$n = E_b/E_s$
Case 3	1	20	10
Case 4	1	20	100

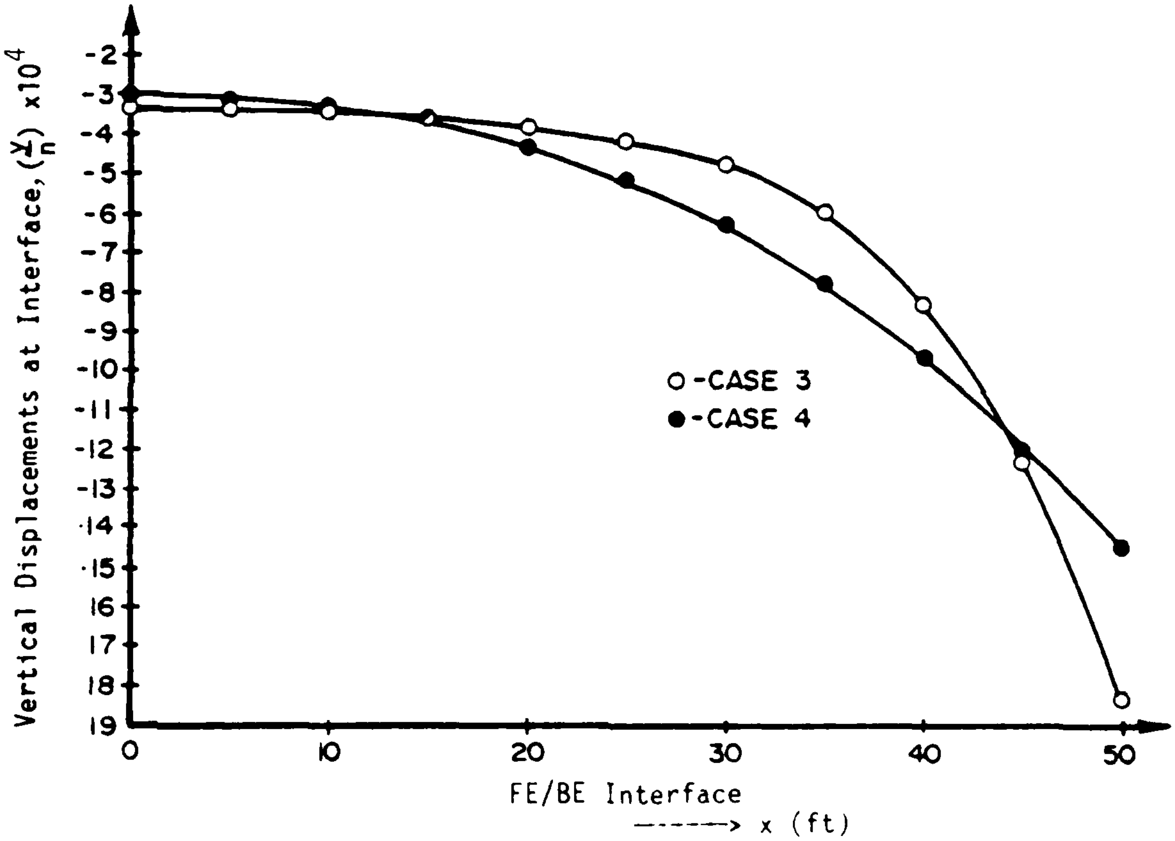

Figure 14a. Vertical displacements at the interface for cases 3 and 4 with concentrated load of 250 k at each end of the beam

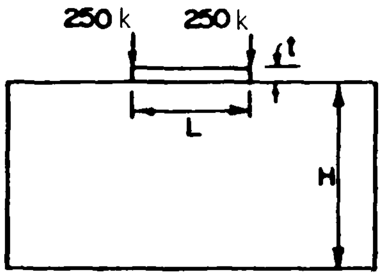

	H/L	L/t	$n = E_b/E_s$
Case 3	1	20	10
Case 4	1	20	100

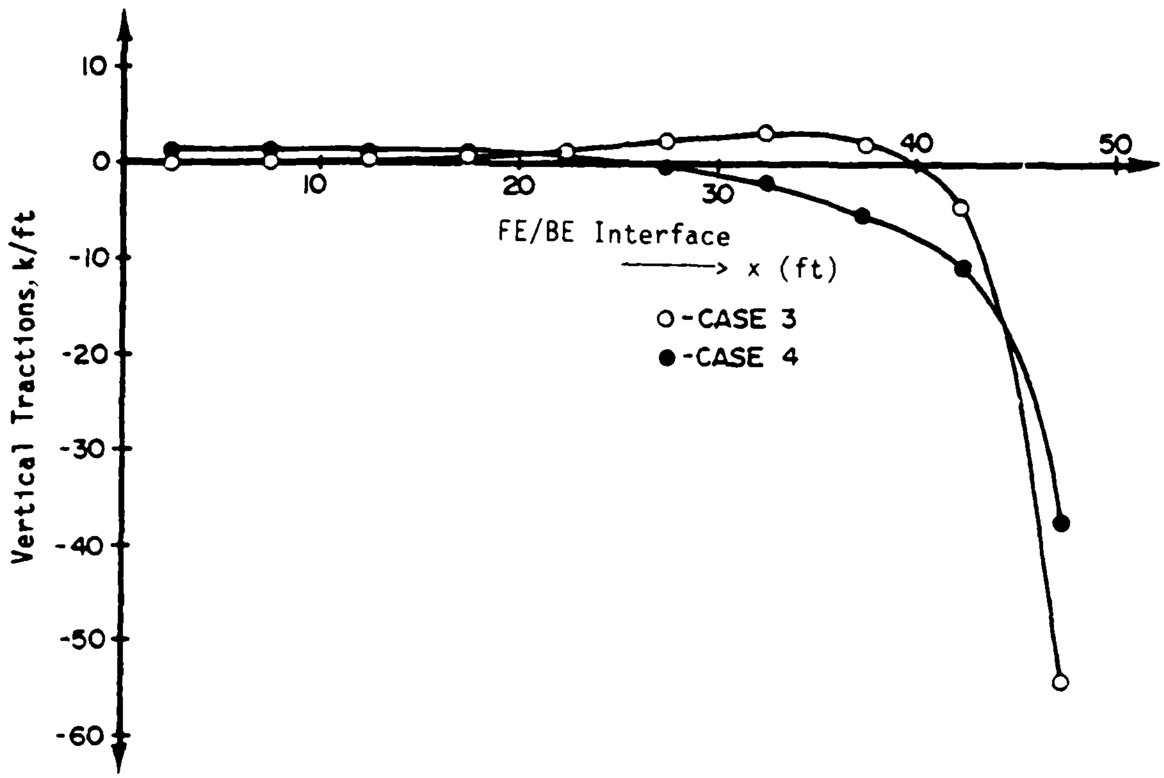

Figure 14b. Vertical tractions at the interface for cases 3 and 4 with concentrated load of 250 k at each end of the beam

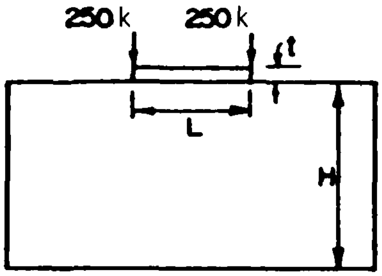

	H/L	L/t	$n = E_b/E_s$
Case 5	2	10	10
Case 6	2	10	100

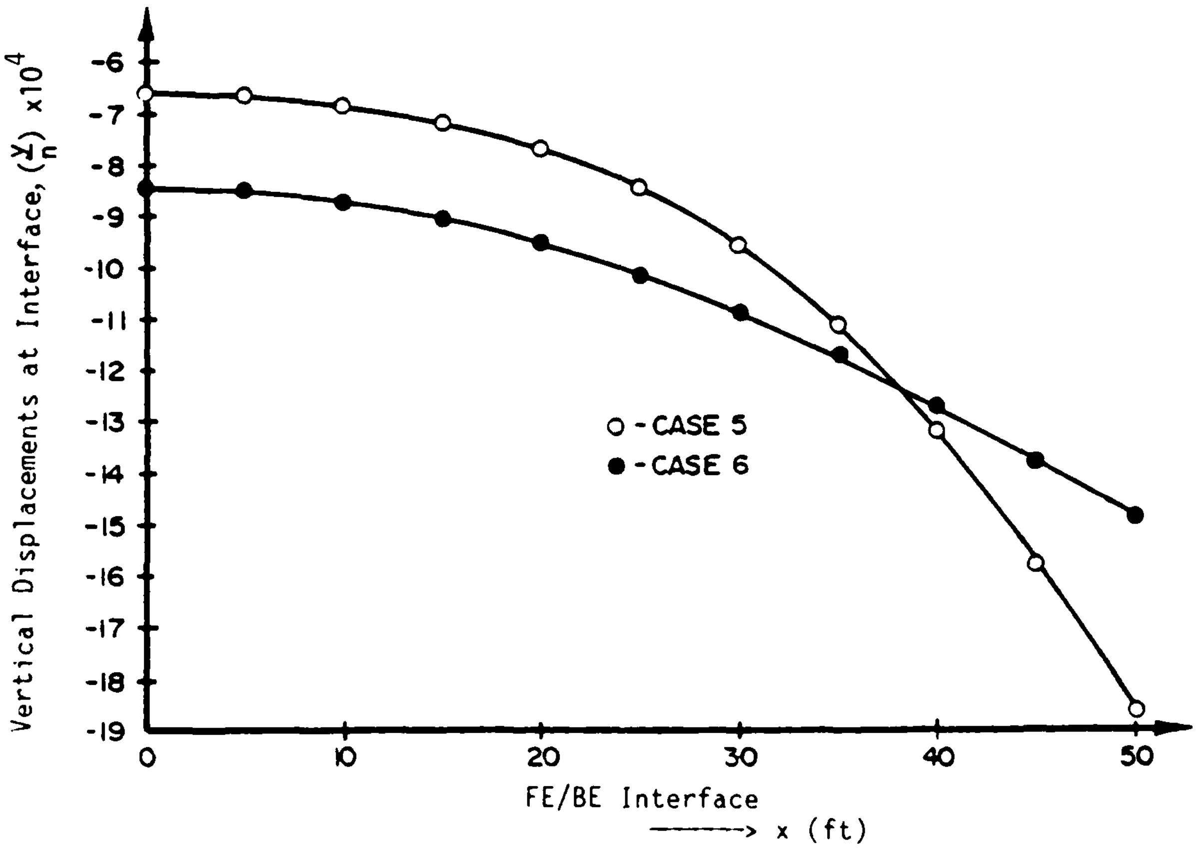

Figure 15a. Vertical displacements at the interface for cases 5 and 6 with concentrated load of 250 k at each end of the beam

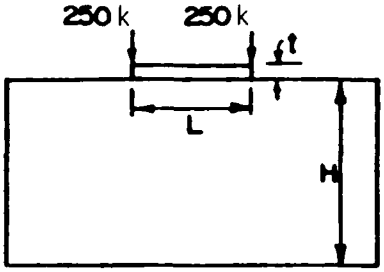

	H/L	L/t	$n = E_b/E_s$
Case 5	2	10	10
Case 6	2	10	100

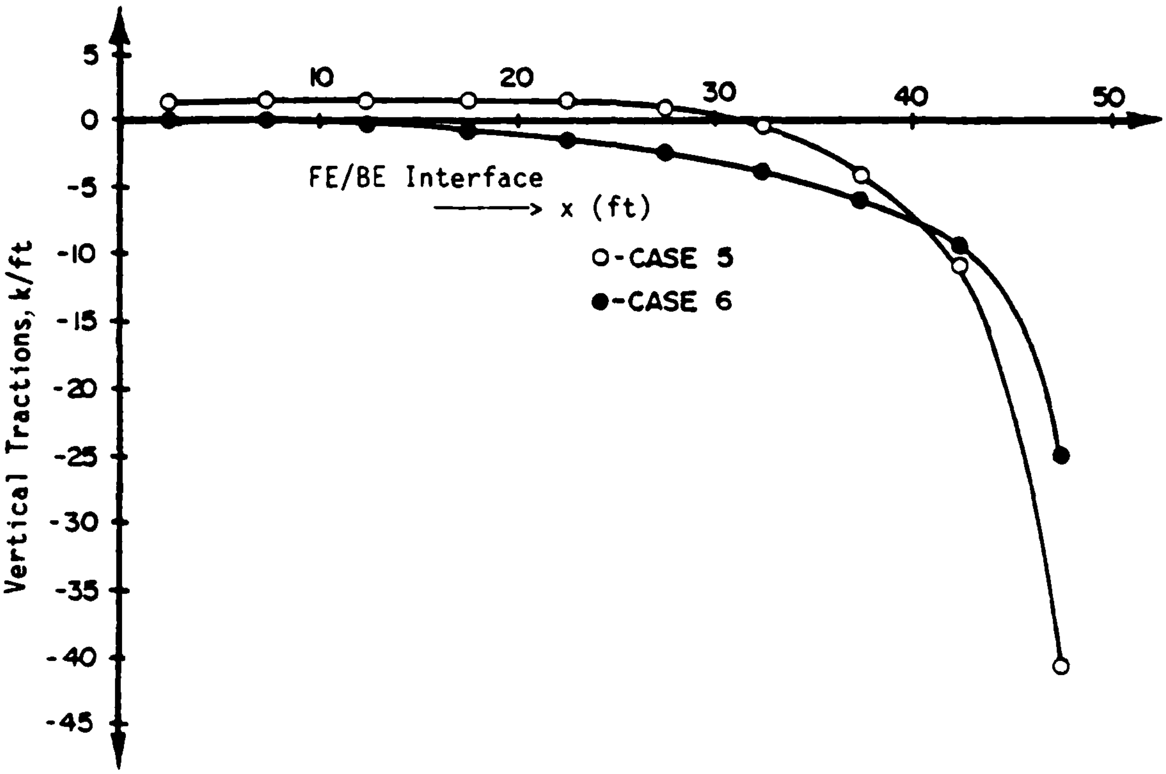

Figure 15b. Vertical tractions at the interface for cases 5 and 6 with concentrated load of 250 k at each end of the beam

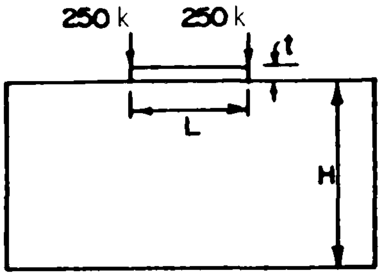

	H/L	L/t	n = E_b/E_s
Case 7	2	20	10
Case 8	2	20	100

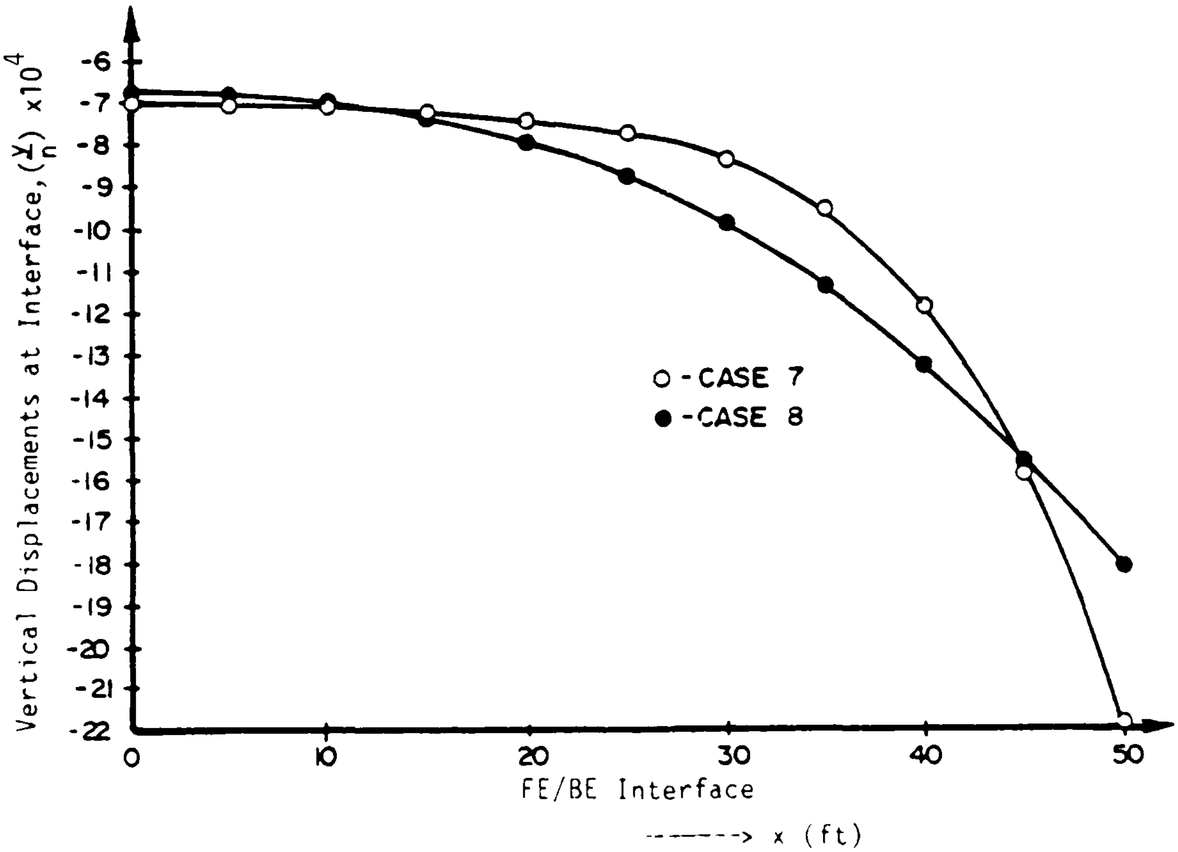

Figure 16a. Vertical displacements at the interface for cases 7 and 8 with concentrated load of 250 k at each end of the beam

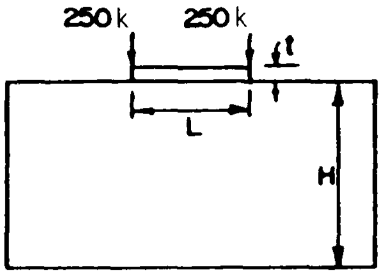

	H/L	L/t	$n = E_b/E_s$
Case 7	2	20	10
Case 8	2	20	100

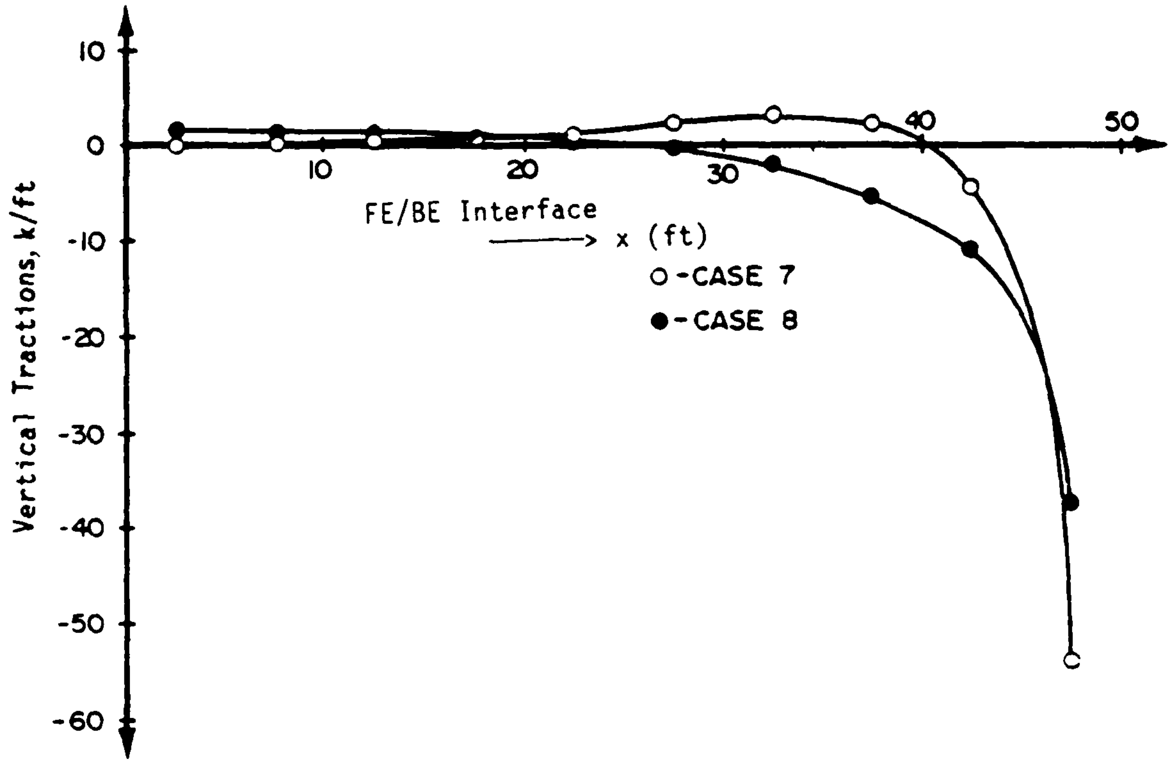

Figure 16b. Vertical tractions at the interface for cases 7 and 8 with concentrated load of 250 k at each end of the beam

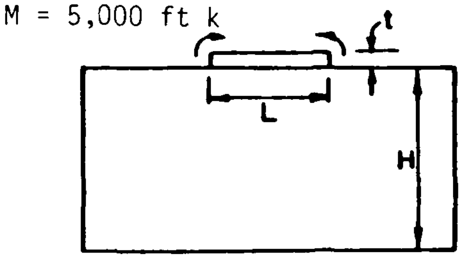

	H/L	L/t	n = E_b/E_s
Case 1	1	10	10
Case 2	1	10	100

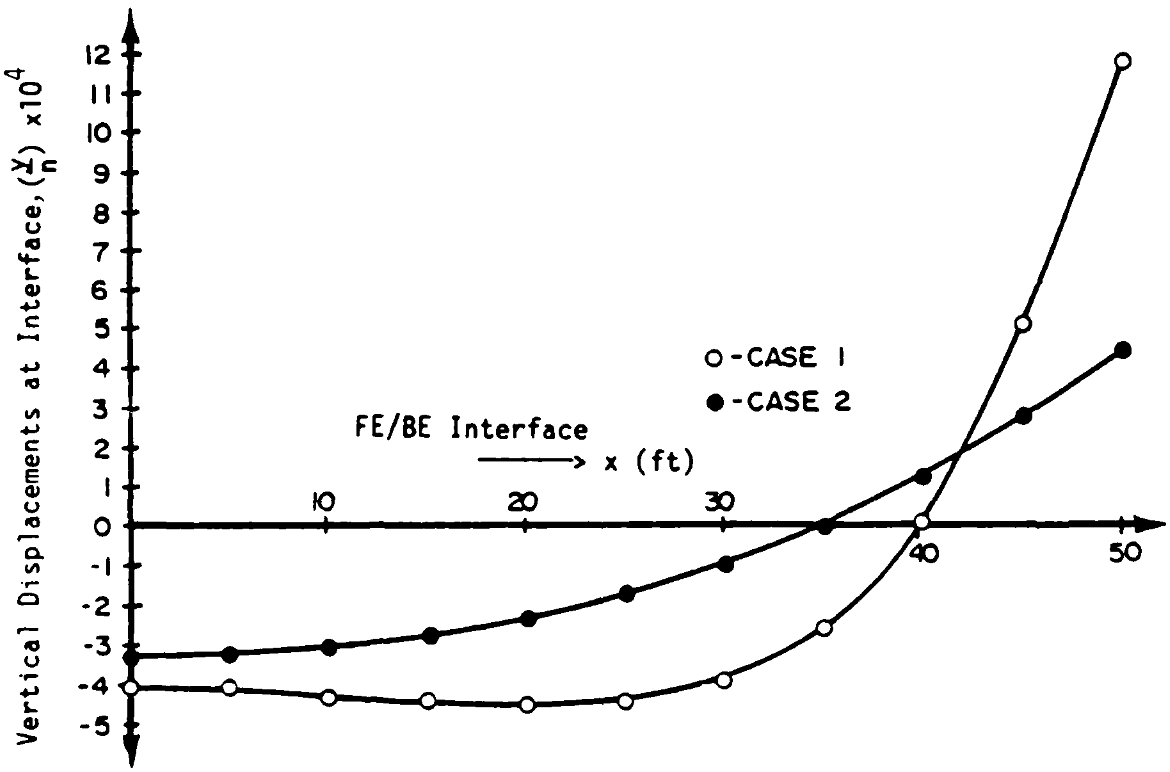

Figure 17a. Vertical displacements at the interface for cases 1 and 2 with concentrated moment of 5,000 ft-k at end end of beam

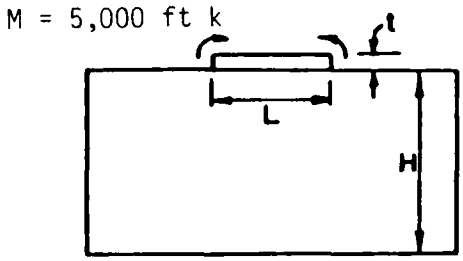

	H/L	L/t	$n = E_b/E_s$
Case 1	1	10	10
Case 2	1	10	100

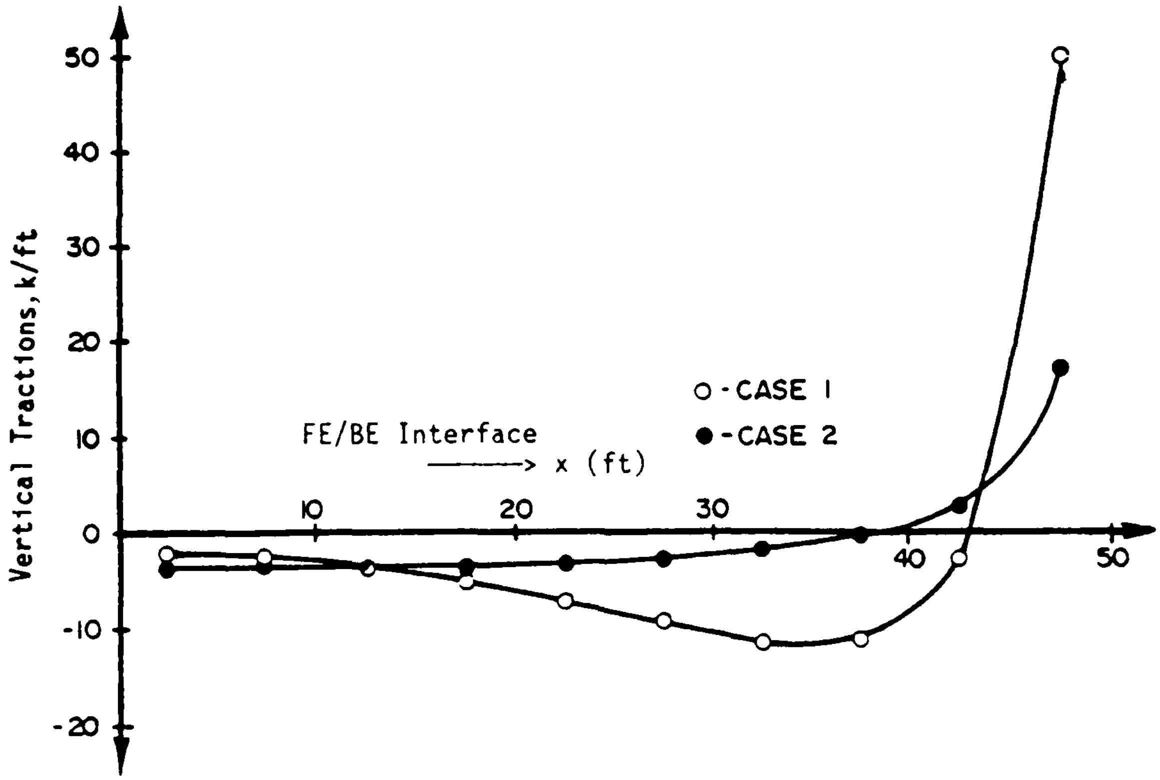

Figure 17b. Vertical tractions at the interface for cases 1 and 2 with concentrated moment of 5,000 ft-k at each end of beam

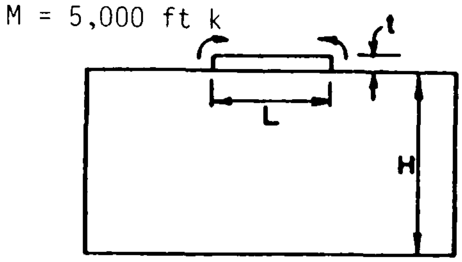

	H/L	L/t	$n = E_b/E_s$
Case 3	1	20	10
Case 4	1	20	100

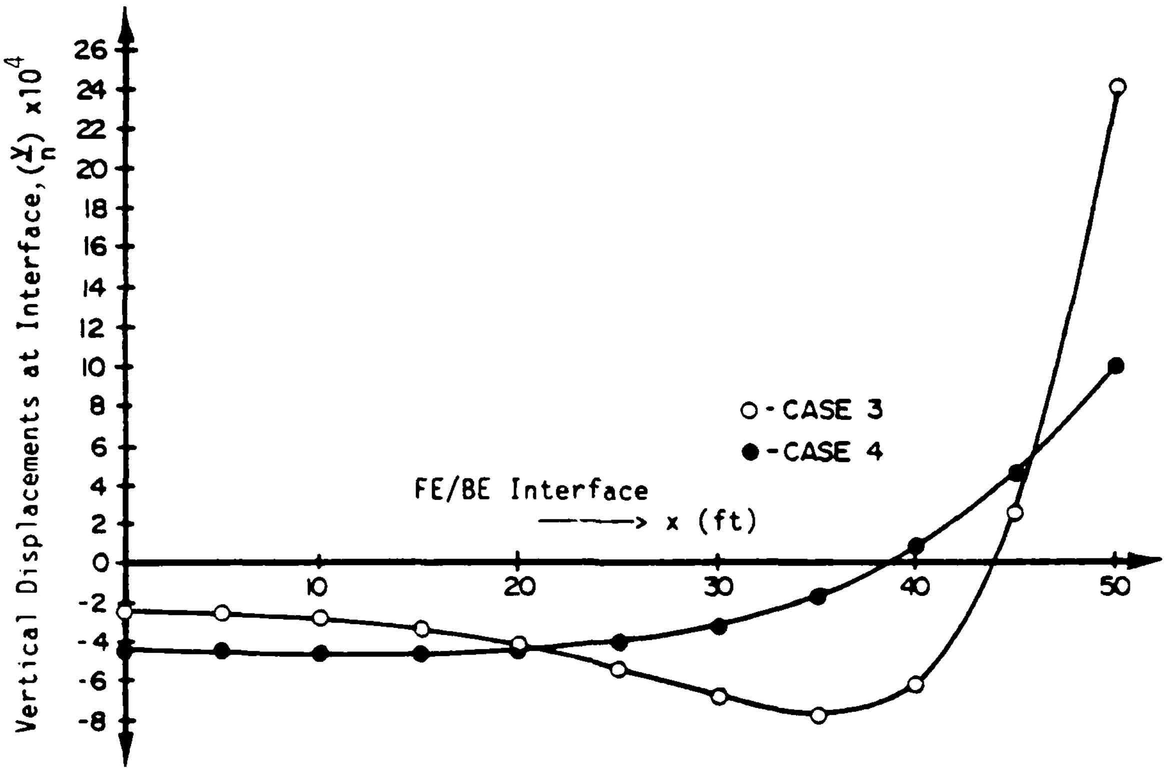

Figure 18a. Vertical displacements at the interface for cases 3 and 4 with concentrated moment of 5,000 ft-k at each end of beam

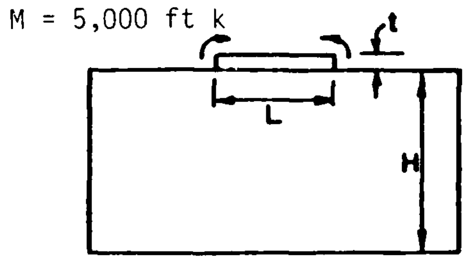

	H/L	L/t	$n = E_b/E_s$
Case 3	1	20	10
Case 4	1	20	100

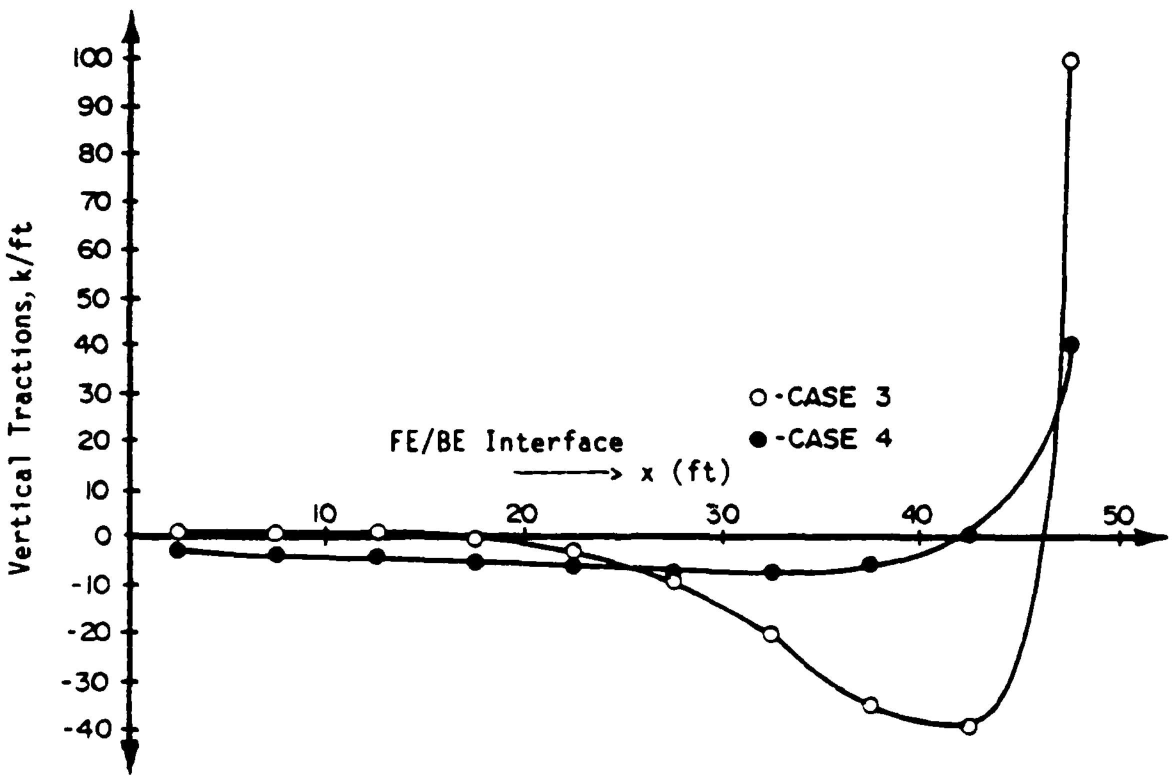

Figure 18b. Vertical tractions at the interface for cases 3 and 4 with concentrated moment of 5,000 ft-k at each end of beam

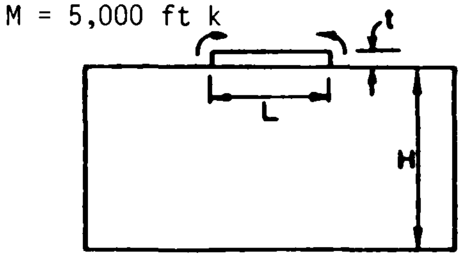

	H/L	L/t	$n = E_b/E_s$
Case 5	2	10	10
Case 6	2	10	100

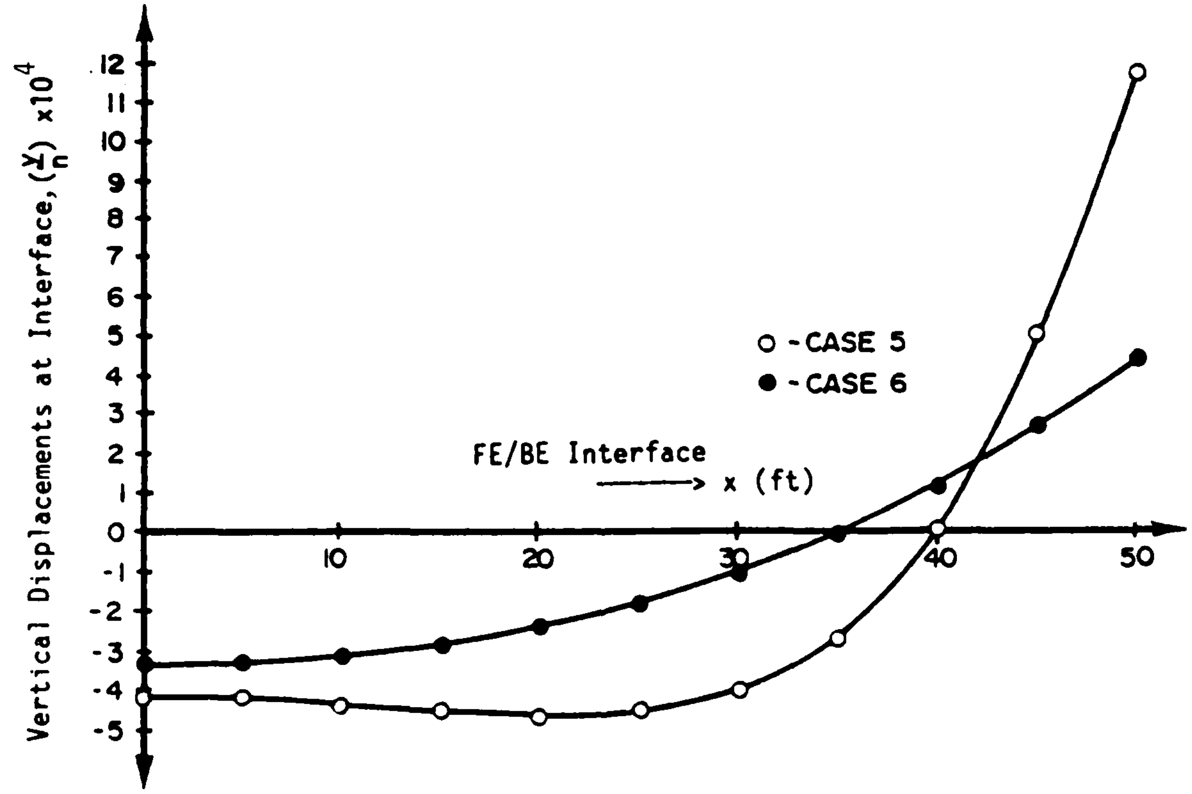

Figure 19a. Vertical displacements at the interface for cases 5 and 6 with concentrated moment of 5,000 ft-k at each end of beam

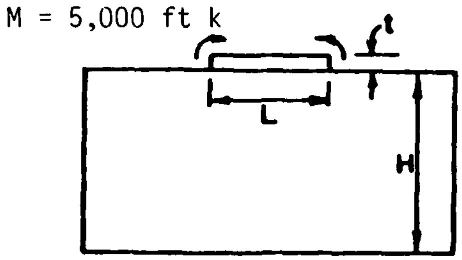

	H/L	L/t	n = E_b/E_s
Case 5	2	10	10
Case 6	2	10	100

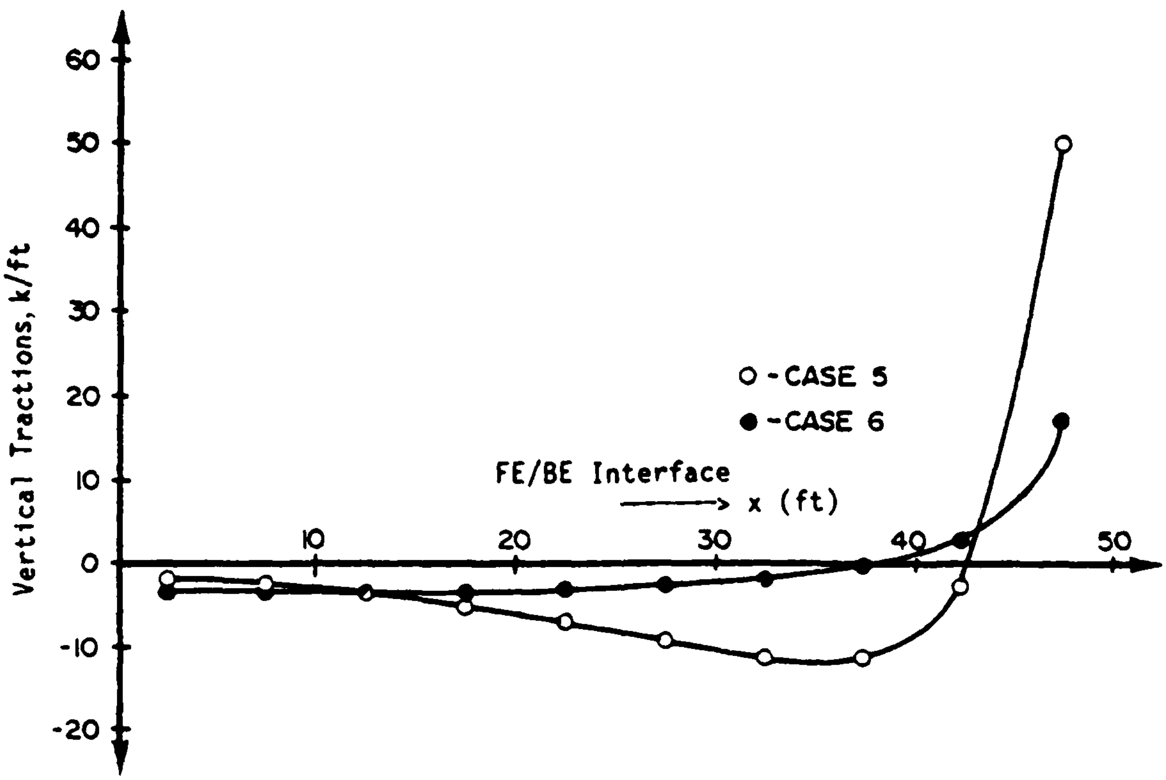

Figure 19b. Vertical tractions at the interface for cases 5 and 6 with concentrated moment of 5,000 ft-k at each end of beam

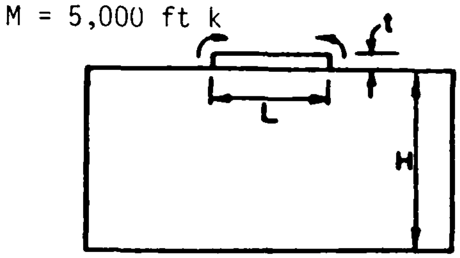

	H/L	L/t	$n = E_b/E_s$
Case 7	2	20	10
Case 8	2	20	100

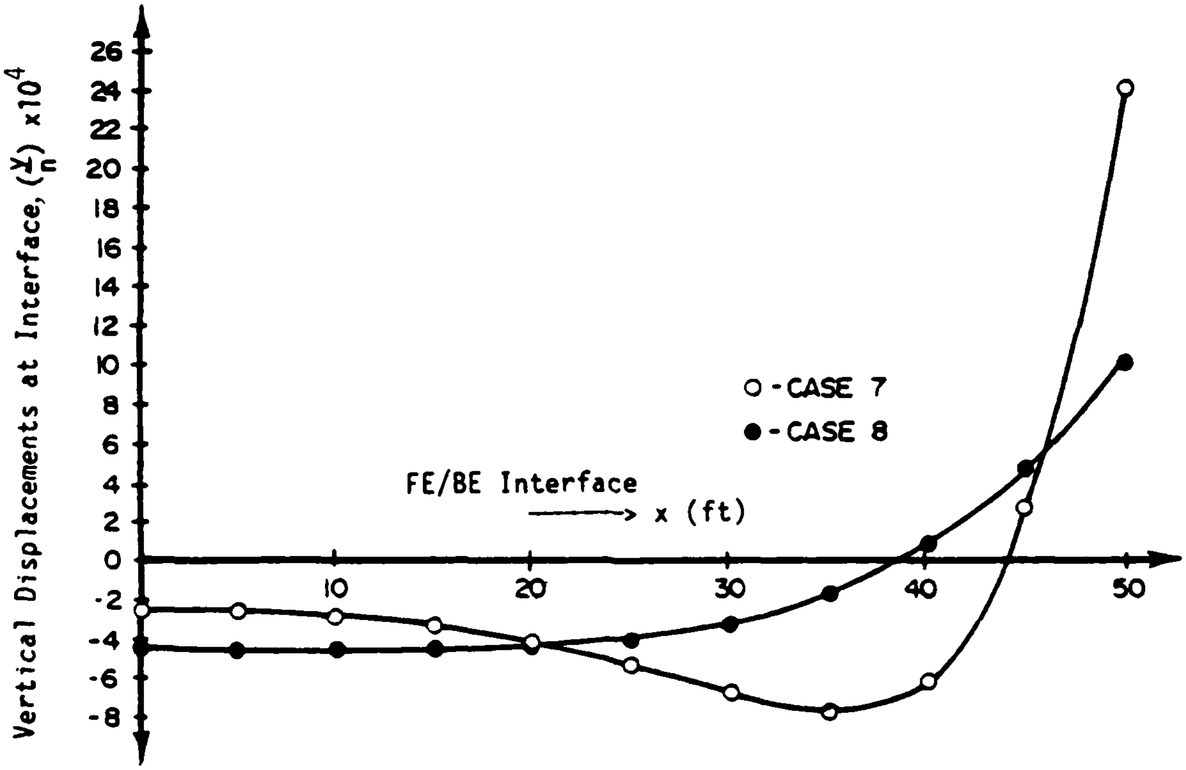

Figure 20a. Vertical displacements at the interface for cases 7 and 8 with concentrated moment of 5,000 ft-k at each end of beam

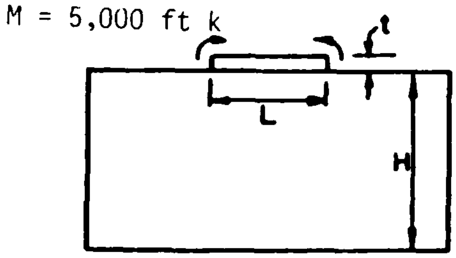

	H/L	L/t	$n = E_b/E_s$
Case 7	2	20	10
Case 8	2	20	100

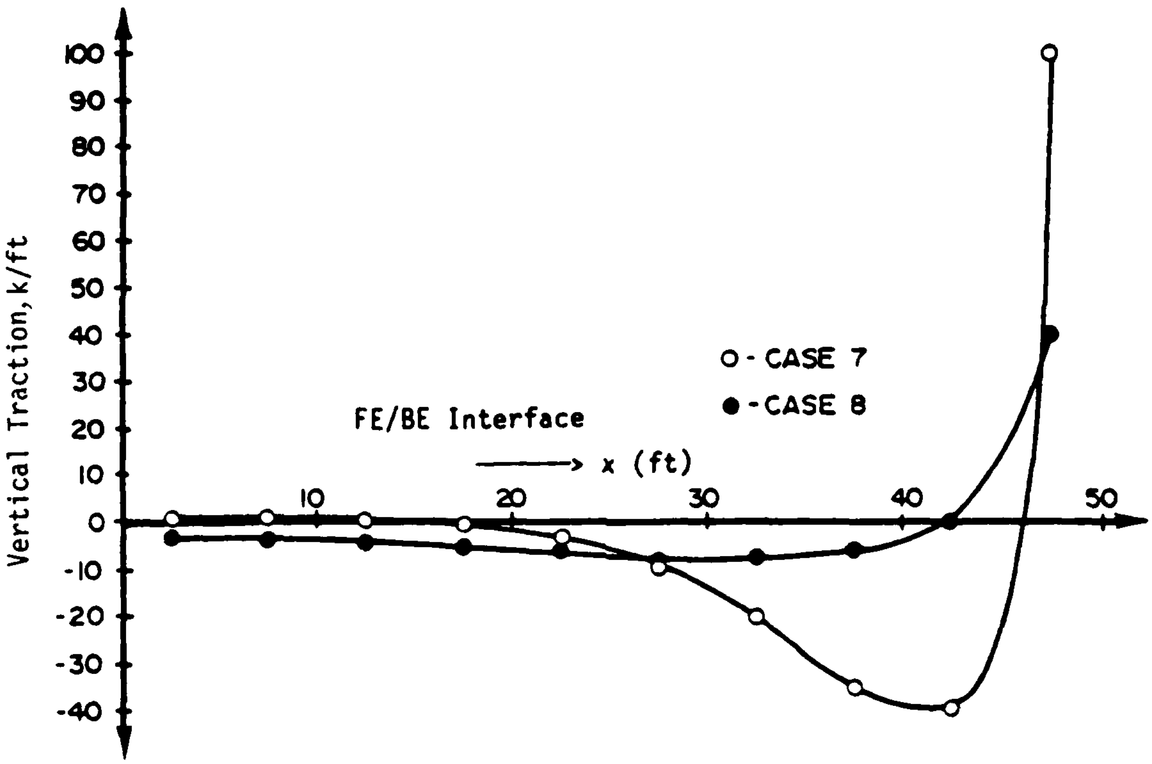

Figure 20b. Vertical tractions at the interface for cases 7 and 8 with concentrated moment of 5,000 ft-k at each end of beam

displacements at the interface and Tables A-2, A-4, and A-6 display the vertical tractions at the interface for the first category. It is in this category that the horizontal displacements at the soil interface are neglected. Similarly, vertical displacements and tractions at the interface for the second category are listed in Tables B-1 through B-6. The compatibility of the vertical and horizontal displacements of the soil at the interface are enforced in this category. The results of the complete finite-element study for cases 5, 6, 7, and 8 for $H/L = 2$ for each loading condition are shown in Tables C-1 through C-3. Here, only the displacements of the soil-structure interface are shown.

41. The comparisons of interface displacements obtained from the finite-element analysis for cases 5, 6, 7, and 8 for $H/L = 2$ for each loading condition are made with the corresponding cases in the coupled FE/BE model of the second category. The horizontal displacements of the soil interface are also included in the analysis and the plots are shown in Figures 21 through 26.

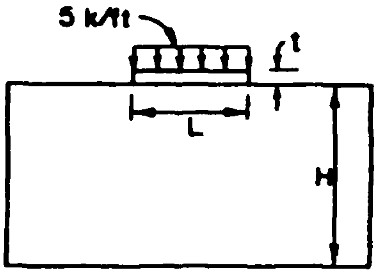

	H/L	L/t	$n = E_b/E_s$
Case 5	2	10	10
Case 6	2	10	100

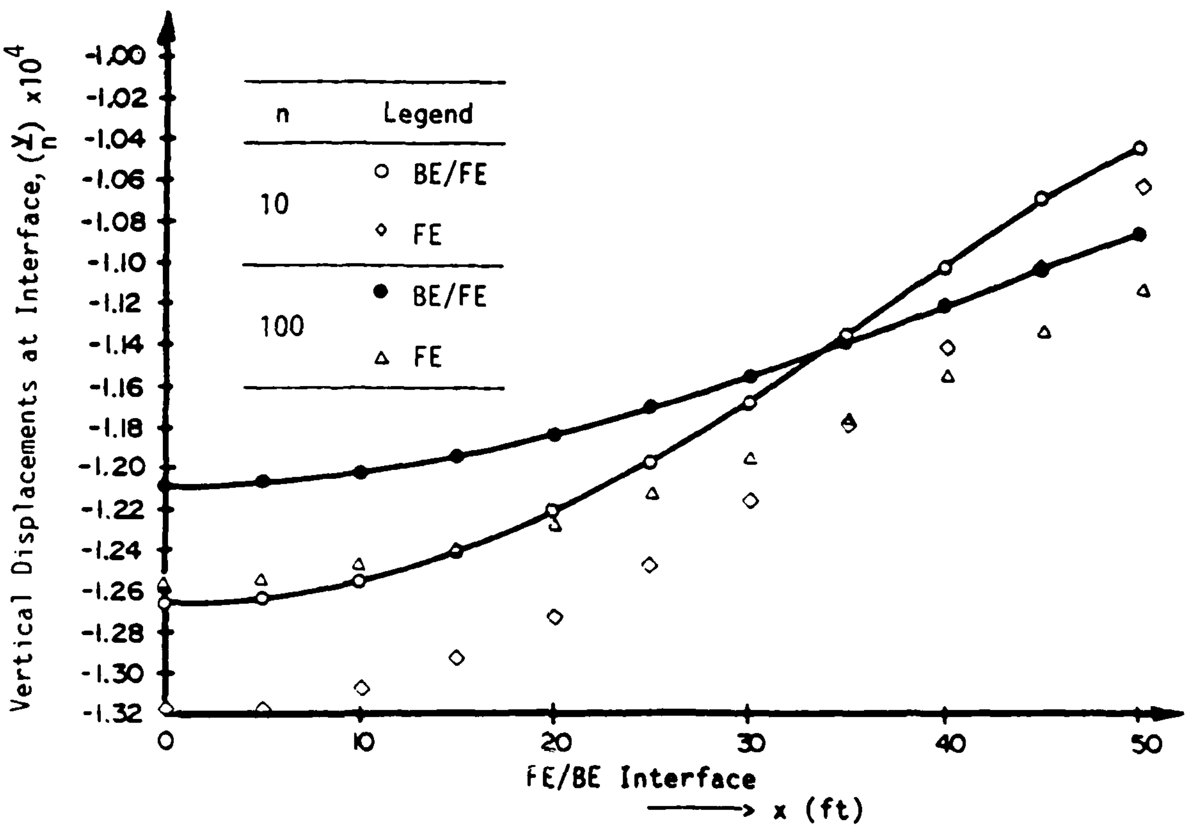

Figure 21. Comparison of displacements at the interface for cases 5 and 6 with uniformly distributed load 5 k/ft on top of beam

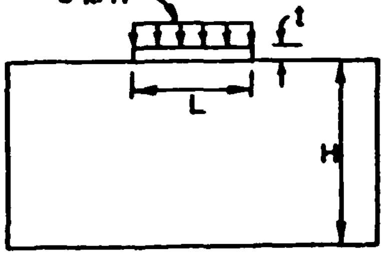

	H/L	L/t	$n = E_b/E_s$
Case 7	2	20	10
Case 8	2	20	100

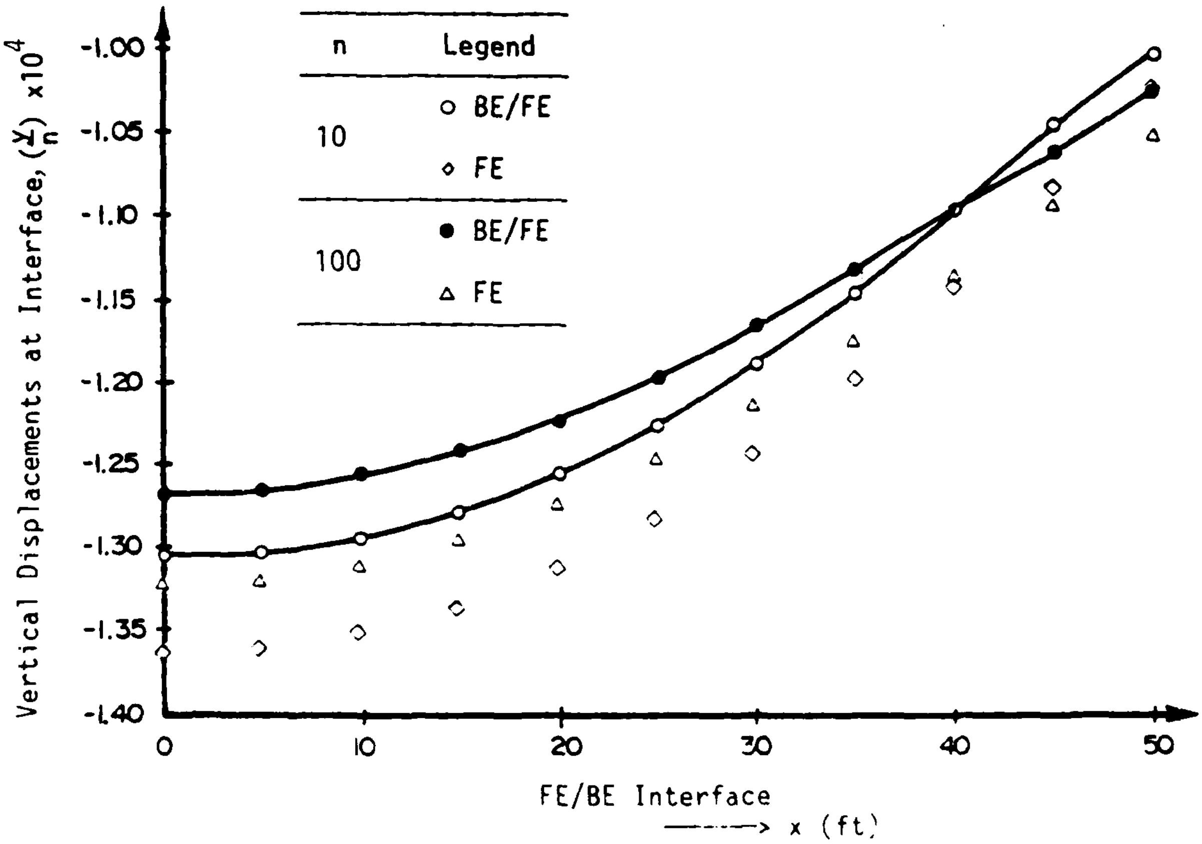

Figure 22. Comparison of displacements at the interface for cases 7 and 8 with uniformly distributed load 5 k/ft on top of beam

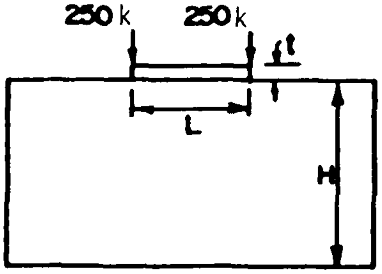

	H/L	L/t	$n = E_b/E_s$
Case 5	2	10	10
Case 6	2	10	100

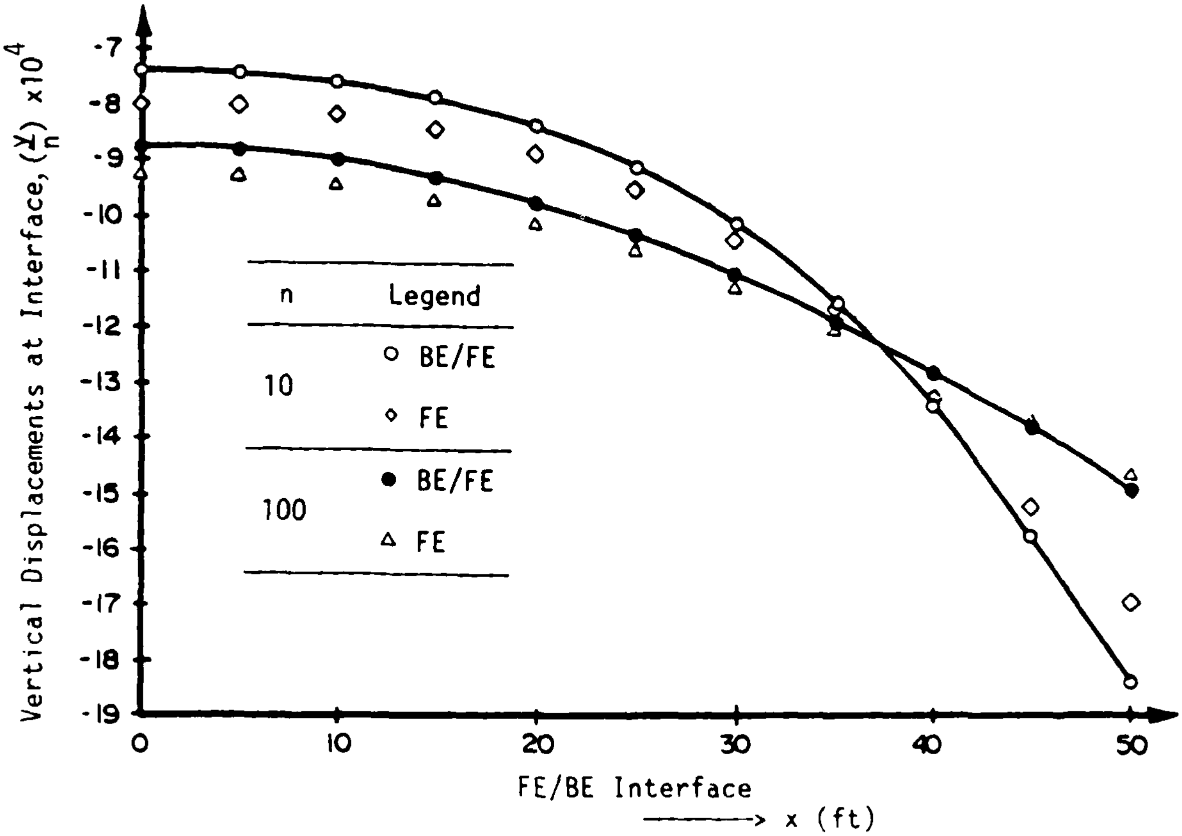

Figure 23. Comparison of displacements at the interface for cases 5 and 6 with a concentrated load of 250 k at each end of the beam

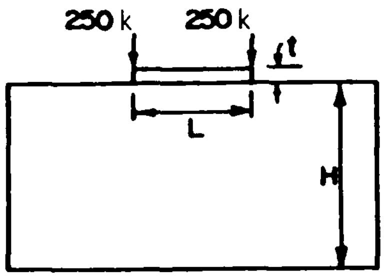

	H/L	L/t	$n = E_b/E_s$
Case 7	2	20	10
Case 8	2	20	100

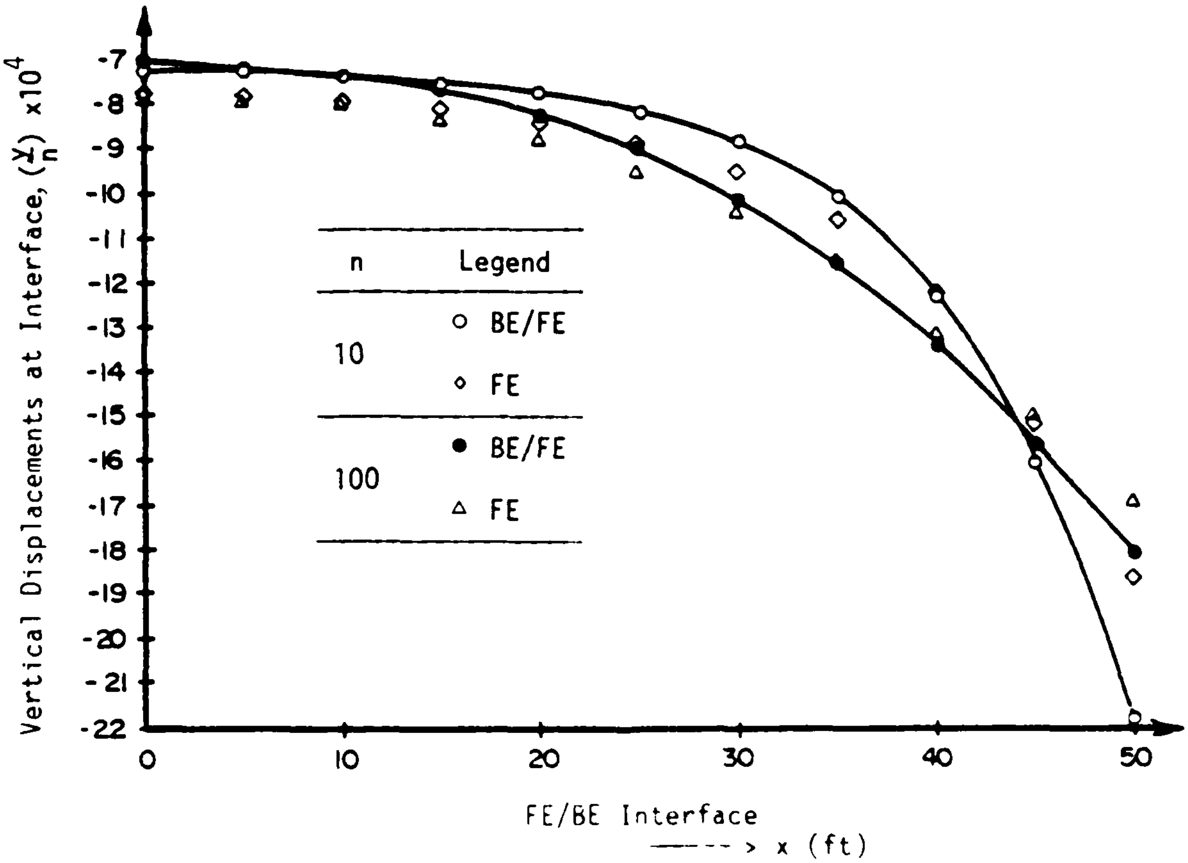

Figure 24. Comparison of displacements at the interface for cases 7 and 8 with a concentrated load of 250 k at each end of beam

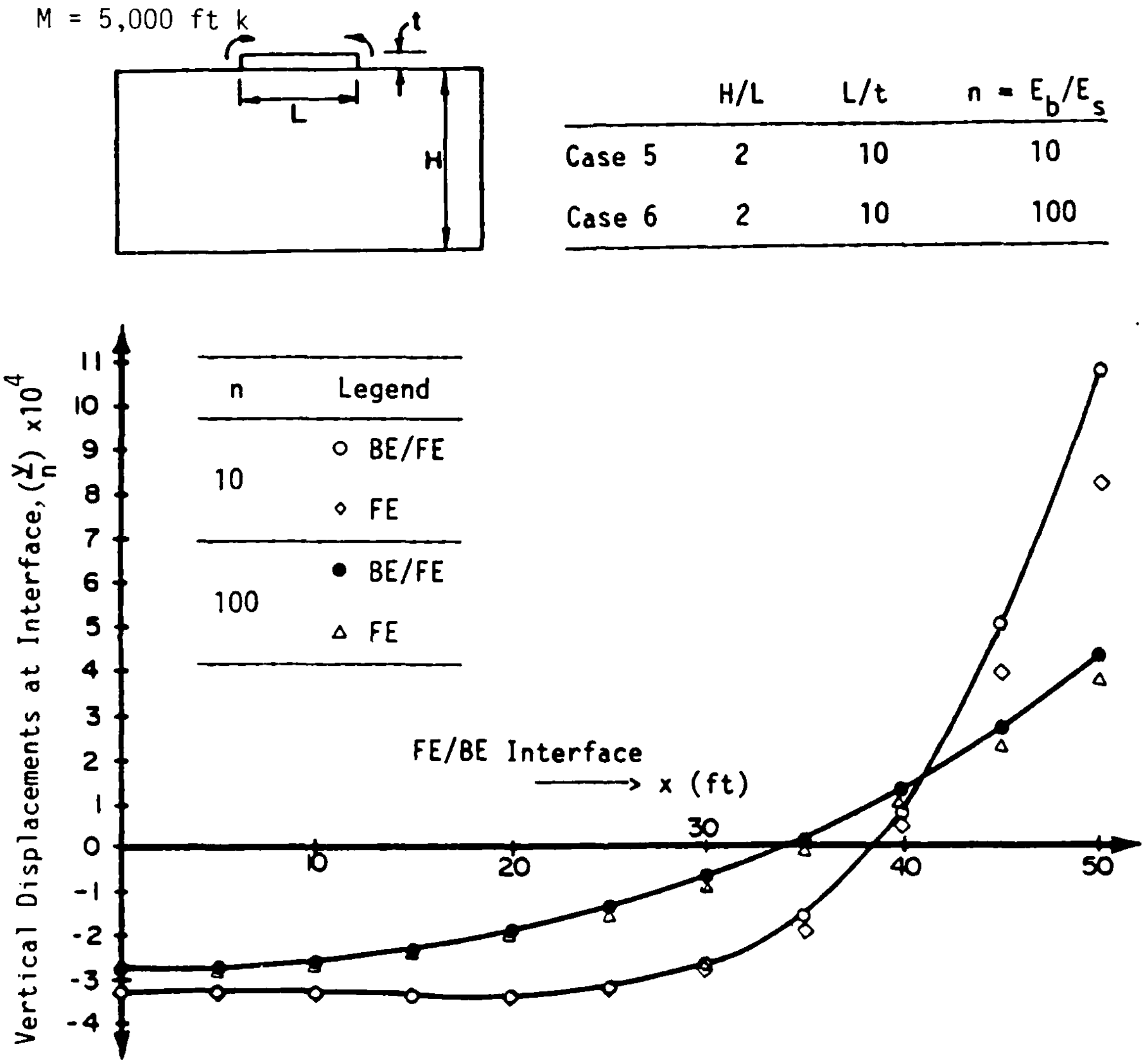

	H/L	L/t	$n = E_b/E_s$
Case 5	2	10	10
Case 6	2	10	100

Figure 25. Comparison of displacements at the interface for cases 5 and 6 with a concentrated moment of 5,000 ft-k at each end of beam

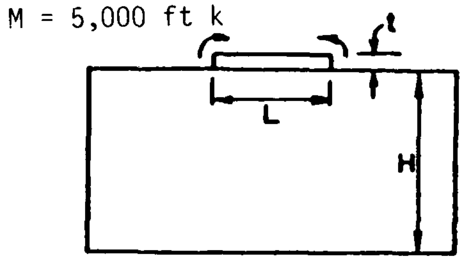

	H/L	L/t	$n = E_b/E_s$
Case 7	2	20	10
Case 8	2	20	100

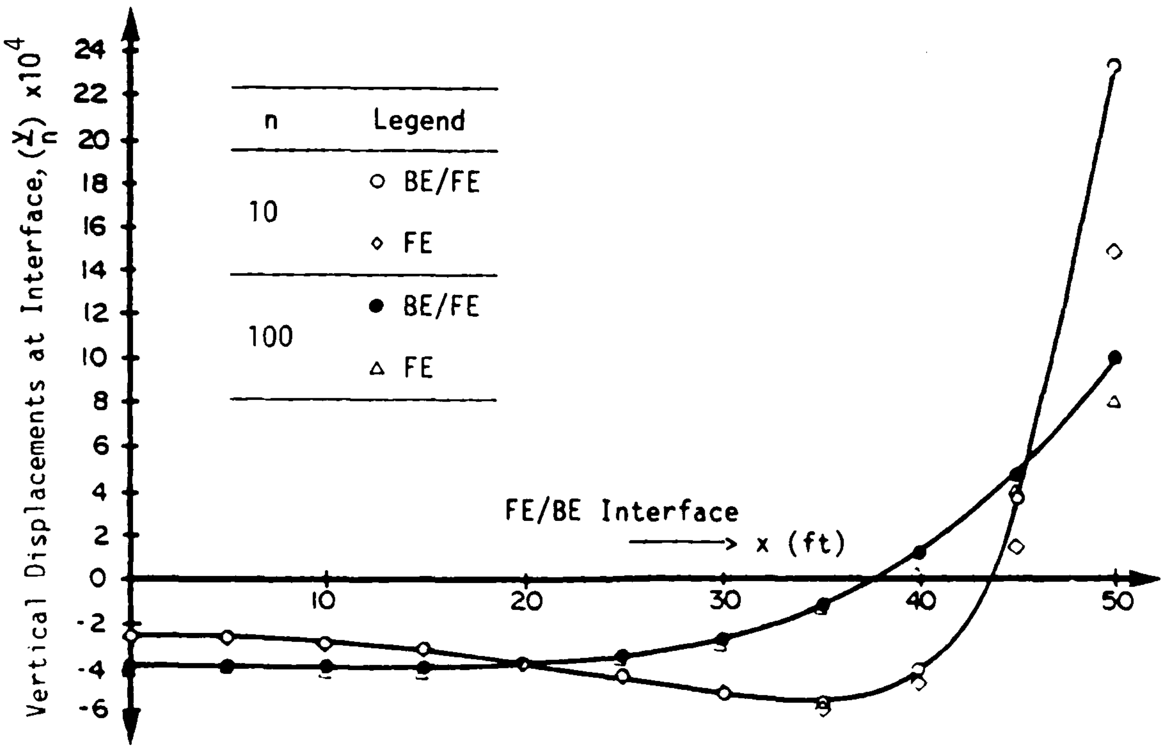

Figure 26. Comparison of displacements at the interface for cases 7 and 8 with a concentrated moment of 5,000 ft-k at each end of beam

PART V: SUMMARY AND CONCLUSIONS

Summary and Findings

42. The feasibility study of the boundary-element technique for stress analysis of soil media was made by Vallabhan (1983). Based on promising results for elastostatic problems, the research was continued for application specifically in soil-structure interaction problems. Here, the structure is modeled by the BEM and the soil is modeled by the FEM. Since the soil is considered as a two-dimensional plane-strain problem, the boundary consists of lines and input data for these problems are extremely simple. A model problem suggested by the Waterways Experiment Station has been solved. Results are compared with full finite-element solutions. The comparisons are very good.

43. Since the methodology and the equations obtained from these two numerical methods are different, the emphasis on this research was to develop a convenient and economical technique to couple the two methods of analysis for solving soil-structure interaction problems. Using a static condensation procedure, the boundary-element equations are reduced and transformed into a stiffness matrix on the interface boundary between the structure and the soil medium. This way the properties of the half-band width of the finite-element stiffness matrix is preserved. A computer code for the coupling of the two methods has been developed in FORTRAN.

Conclusions

44. The following conclusions are made from this study:

  a. The results of the FEM/BE combined model compare very well with the full FEM model for the soil and the structure.

  b. The coupling method developed here is found to be very efficent in numerical computation and in preparation of input data.

  c. Constant boundary elements are employed here. The stiffness matrix computed using constant boundary elements is almost symmetric and the maximum error in lack of symmetry when compared to the diagonal elements for the above problem is less than 0.002 percent.

REFERENCES

Banerjee, P. K., and Butterfield, R. 1981. Boundary Element Methods in Engineering Science, McGraw-Hill, London.

Brebbia, C. A., and Walker, S. 1972. Introduction to Boundary Element Methods, Pentech Press, London.

Brebbia, C. A., Telles, J. C. F., and Wrobel, L. C. 1984. Boundary Element Techniques Theory and Application in Engineering, Springer-Verlag, New York.

Crouch, S. L., and Starfield, A. M. 1983. Boundary Element Methods in Solid Mechanics, Allen and Unwin, London.

Duncan, J. M., and Clough, G. W. 1971. "Finite Element Analysis of Port Allen Lock," Journal, Soil Mechanics and Foundations Division, American Society of Civil Engineers, Vol 77, No. SM8.

Georgiou, P. 1981. The Coupling of the Direct Boundary Element Method with the Finite Element Displacement Technique in Elastostatics, Ph. D. Dissertation, Southampton University.

Hartmann, F. 1981. "The Derivation of Stiffness Matrices from Integral Equations," Boundary Element Methods, C. A. Brebbia, ed., Springer-Verlag, Berlin.

Hetenyi, M. 1946. "Beams on Elastic Foundation," University of Michigan Press, Ann Arbor, Mich.

Love, A. E. H. 1927. Treatise on the Mathematical Theory of Elasticity, Dover Press.

Matlock, H., and Reese, L. C. 1960 (Dec). "Generalized Solutions for Laterally-Loaded Piles," Proceedings, American Society of Civil Engineers, Vol 86, No. SM5, pp 63-91.

Pasternak, P. L. 1954. On a New Method of Analysis of an Elastic Foundation by Means of Two Foundation Constants, Gos. Izd. Lit. Postroiti Arkh., Moscow.

Scott, R. F. 1981. Foundation Analysis, Prentice-Hall, New Jersey.

Terzaghi, K. 1955. "Evaluation of Coefficients of Subgrade Reaction," Geotechnique, Vol 5, p 297.

Vallabhan, C. V. G. 1983 (Sep). "A Feasiblity Study of Boundary Element for Soil-Structure Interaction Problems," report for US Army Engineer Waterways Experiment Station, Vicksburg, Miss.

Vallabhan, C. V. G., and Jain, R. K. 1972 (May). "Octahedral Stress Approach to Analysis of Water Resources Structures," Proceedings, Symposium on Application of Finite Element Method in Geotechnical Engineering, Vicksburg, Miss.

Vesic, A. S. 1961 (Apr). "Bending of Beams Resting on Isotropic Elastic Solid," Journal, Engineering Mechanics Division, American Society of Civil Engineers, Vol 87, No. EM2, p 35.

Westergaard, H. M. 1926. "Stresses on Concrete Pavements Computed by Theoretical Analysis," Public Roads, Vol 7, No. 25.

Wilson, E. L. 1974. "The Static Condensation Algorithm," International Journal of Numerical Methods in Engineering, Vol 8, pp 199-203.

BIBLIOGRAPHY

Chaudonneret, M. 1978. "On the Discontinuity of the Stress Vector in the Boundary Integral Equation Method for Elastic Analysis," Recent Advances in Boundary Element Methods, C. A. Brebbia, ed., Pentech Press, London.

Mindlin, R. D. 1936. "Force at a Point in the Interior of A Semi-infinite Solid," Journal of Physics, Vol 7.

Vallabhan, C. V. G., Sivakumar, J., and Radhakrishnan, N. 1984 (Jul). "Application of Boundary Element Method for Soil-Structure Interaction Problems," Proceeding of Sixth International Conference on Boundary Element Methods.

Zienkiewicz, O. C. 1967. The Finite Element Method, McGraw-Hill, New York.

Table 1

Nomenclature for Eight Loading Cases of Beam/Soil Geometry and Material Properties

Case	Foundation Depth, ft	Beam Depth ft	Modular Ratio $n = \frac{E_b}{E_s}$
1	100	10	10
2	100	10	100
3	100	5	10
4	100	5	100
5	200	10	10
6	200	10	100
7	200	5	10
8	200	5	100

APPENDIX A: VERTICAL DISPLACEMENTS AND TRACTIONS AT INTERFACE, CATEGORY 1

Table A1

Vertical Displacements at Interface, Loading Case 1

UDL 5 k/ft--Top of Beam

Detail	H/L = 1				H/L = 2			
	L/t = 10		L/t = 20		L/t = 10		L/t = 20	
	$n = E_b/E_s$		$n = E_b/E_s$		$n = E_b/E_s$		$n = E_b/E_s$	
	10	100	10	100	10	100	10	100
Case	1	2	3	4	5	6	7	8
	$\times 10^{-3}$	$\times 10^{-2}$	$\times 10^{-3}$	$\times 10^{-2}$	$\times 10^{-2}$	$\times 10^{-1}$	$\times 10^{-2}$	$\times 10^{-1}$
Node No.								
1	-9.119	-8.554	-9.159	-9.071	-1.293	-1.231	-1.298	-1.287
2	-9.091	-8.535	-9.135	-9.042	-1.290	-1.229	-1.295	-1.284
3	-9.005	-8.478	-9.060	-8.955	-1.280	-1.223	-1.287	-1.275
4	-8.862	-8.385	-8.933	-8.810	-1.265	-1.213	-1.273	-1.259
5	-8.659	-8.257	-8.748	-8.607	-1.243	-1.199	-1.252	-1.237
6	-8.395	-8.099	-8.497	-8.346	-1.214	-1.183	-1.225	-1.209
7	-8.069	-7.912	-8.172	-8.031	-1.180	-1.163	-1.190	-1.176
8	-7.685	-7.703	-7.759	-7.666	-1.139	-1.141	-1.146	-1.137
9	-7.248	-7.477	-7.255	-7.259	-1.093	-1.117	-1.093	-1.094
10	-6.763	-7.240	-6.665	-6.824	-1.042	-1.092	-1.032	-1.048
11	-6.266	-7.000	-6.038	-6.378	-0.990	-1.066	-0.967	-1.002

Note: L = 100 ft , E_b = 432,000 k/ft^2 , ν_b = 0.2 , ν_s = 0.2 .

Table A2

Vertical Tractions at Interface, Loading Case 1

UDL 5 k/ft--Top of Beam

Detail	H/L = 1				H/L = 2			
	L/t = 10		L/t = 20		L/t = 10		L/t = 20	
	$n = E_b/E_s$		$n = E_b/E_s$		$n = E_b/E_s$		$n = E_b/E_s$	
	10	100	10	100	10	100	1C	100
Case	1	2	3	4	5	6	7	8
	$\times 10^1$	$\times 10^1$	$\times 10^1$	$\times 10^1$	$\times 10^1$	$\times 10^1$	$\times 10^1$	$\times 10^1$
Element No.								
1	-0.517	-0.453	-0.508	-0.507	-0.517	-0.447	-0.509	-0.506
2	-0.515	-0.451	-0.509	-0.505	-0.515	-0.445	-0.509	-0.503
3	-0.512	-0.448	-0.509	-0.500	-0.512	-0.443	-0.510	-0.499
4	-0.507	-0.445	-0.510	-0.493	-0.506	-0.441	-0.510	-0.492
5	-0.498	-0.442	-0.510	-0.483	-0.498	-0.439	-0.510	-0.482
6	-0.487	-0.441	-0.507	-0.471	-0.487	-0.441	-0.507	-0.471
7	-0.472	-0.446	-0.499	-0.458	-0.473	-0.448	-0.498	-0.460
8	-0.460	-0.466	-0.481	-0.450	-0.463	-0.473	-0.483	-0.454
9	-0.453	-0.512	-0.454	-0.455	-0.461	-0.526	-0.460	-0.465
10	-0.625	-0.914	-0.545	-0.694	-0.617	-0.918	-0.537	-0.687

Note: L = 100 ft , E_b = 432,000 k/ft^2 , ν_b = 0.2 , ν_s = 0.2 .

Table A3

Vertical Displacements at Interface, Loading Case 2

Point Load 250 k--Beam Ends

Detail	H/L = 1				H/L = 2			
	L/t = 10		L/t = 20		L/t = 10		L/t = 20	
	$n = E_b/E_s$		$n = E_b/E_s$		$n = E_b/E_s$		$n = E_b/E_s$	
	10	100	10	100	10	100	10	100
Case	1	2	3	4	5	6	7	8
	$\times 10^{-3}$	$\times 10^{-2}$	$\times 10^{-3}$	$\times 10^{-2}$	$\times 10^{-3}$	$\times 10^{-2}$	$\times 10^{-3}$	$\times 10^{-2}$
Node No.								
1	-2.924	-4.748	-3.328	-2.953	-6.616	-8.443	-7.028	-6.644
2	-2.983	-4.817	-3.354	-3.028	-6.674	-8.511	-7.051	-6.717
3	-3.169	-5.024	-3.430	-3.258	-6.854	-8.714	-7.120	-6.941
4	-3.508	-5.368	-3.564	-3.663	-7.182	-9.053	-7.242	-7.337
5	-4.043	-5.850	-3.776	-4.275	-7.703	-9.527	-7.439	-7.936
6	-4.835	-6.466	-4.130	-5.135	-8.478	-10.130	-7.773	-8.780
7	-5.964	-7.214	-4.770	-6.292	-9.588	-10.870	-8.392	-9.921
8	-7.523	-8.087	-5.984	-7.795	-11.130	-11.730	-9.583	-11.410
9	-9.636	-9.076	-8.293	-9.681	-13.220	-12.710	-11.870	-13.270
10	-12.230	-10.150	-12.310	-11.950	-15.790	-13.780	-15.870	-15.520
11	-15.090	-11.260	-18.320	-14.490	-18.640	-14.870	-21.870	-18.070

Note: L = 100 ft , E_b = 432,000 k/ft^2 , ν_b = 0.2 , ν_s = 0.2 .

Table A4

Vertical Tractions at Interface, Loading Case 2

Point Load 250 k--Beam Ends

Detail	H/L = 1				H/L = 2			
	L/t = 10		L/t = 20		L/t = 10		L/t = 20	
	$n = E_b/E_s$		$n = E_b/E_s$		$n = E_b/E_s$		$n = E_b/E_s$	
	10	100	10	100	10	100	10	100
Case	1	2	3	4	5	6	7	8
Element No.								
1	1.34	0.09	0.02	1.49	1.37	0.17	0.02	1.51
2	1.40	-0.04	0.09	1.46	1.43	0.02	0.09	1.49
3	1.50	-0.34	0.27	1.38	1.53	-0.28	0.28	1.40
4	1.55	-0.81	0.66	1.16	1.58	-0.77	0.67	1.18
5	1.42	-1.50	1.35	0.69	1.44	-1.47	1.36	0.70
6	0.85	-2.48	2.33	-0.25	0.83	-2.47	2.33	-0.25
7	-0.56	-3.87	3.23	-1.99	-0.57	-3.89	3.23	-2.00
8	-4.07	-6.01	2.23	-5.21	-4.10	-6.07	2.21	-5.25
9	-10.70	-9.23	-4.31	-10.70	-10.80	-9.36	-4.39	-10.80
10	-40.70	-25.00	-54.00	-37.20	-40.70	-25.00	-53.90	-37.10

Note: L = 100 ft , E_b = 432,000 k/ft^2 , ν_b = 0.2 , ν_s = 0.2 .

Table A5

Vertical Displacements at Interface, Loading Case 3

Moment of 5,000 ft-k--Beam Ends

Detail	H/L = 1				H/L = 2			
	L/t = 10		L/t = 20		L/t = 10		L/t = 20	
	$n = E_b/E_s$		$n = E_b/E_s$		$n = E_b/E_s$		$n = E_b/E_s$	
	10	100	10	100	10	100	1C	100
Case	1	2	3	4	5	6	7	8
	$\times 10^{-3}$	$\times 10^{-2}$	$\times 10^{-3}$	$\times 10^{-2}$	$\times 10^{-3}$	$\times 10^{-2}$	$\times 10^{-3}$	$\times 10^{-2}$
Node No.								
1	-4.085	-3.278	-2.457	-4.455	-4.183	-3.334	-2.540	-4.552
2	-4.133	-3.221	-2.529	-4.466	-4.231	-3.277	-2.611	-4.563
3	-4.261	-3.048	-2.770	-4.484	-4.358	-3.103	-2.851	-4.580
4	-4.422	-2.750	-3.248	-4.462	-4.517	-2.805	-3.326	-4.556
5	-4.526	-2.316	-4.060	-4.315	-4.618	-2.370	-4.137	-4.407
6	-4.421	-1.726	-5.272	-3.917	-4.510	-1.780	-5.345	-4.006
7	-3.887	-0.961	-6.722	-3.086	-3.973	-1.013	-6.792	-3.172
8	-2.595	0.055	-7.696	-1.583	-2.678	-0.046	-7.762	-1.665
9	0.142	1.225	-6.155	0.893	0.063	1.175	-6.218	0.814
10	5.104	2.753	2.750	4.778	5.028	2.704	2.690	4.702
11	11.730	4.464	24.130	10.190	11.660	4.417	24.070	10.120

Note: L = 100 ft , E_b = 432,000 k/ft^2 , ν_b = 0.2 , ν_s = 0.2 .

Table A6

Vertical Tractions at Interface, Loading Case 3

Moment of 5,000 ft-k--Beam Ends

Detail	H/L = 1				H/L = 2			
	L/t = 10		L/t = 20		L/t = 10		L/t = 20	
	$n = E_b/E_s$		$n = E_b/E_s$		$n = E_b/E_s$		$n = E_b/E_s$	
	10	100	10	100	10	100	10	100
Case	1	2	3	4	5	6	7	8
Element No.								
1	-2.00	-3.61	0.84	-3.15	-2.03	-3.62	0.82	-3.16
2	-2.51	-3.58	0.82	-3.52	-2.54	-3.59	0.81	-3.53
3	-3.54	-3.49	0.58	-4.23	-3.57	-3.50	0.57	-4.23
4	-5.08	-3.33	-0.43	-5.20	-5.09	-3.33	-0.43	-5.21
5	-7.02	-3.03	-3.24	-6.29	-7.03	-3.03	-3.23	-6.30
6	-9.17	-2.51	-9.30	-7.20	-9.17	-2.52	-9.28	-7.20
7	-11.30	-1.68	-20.20	-7.36	-11.30	-1.68	-20.10	-7.35
8	-11.10	-0.14	-35.30	-5.63	-11.10	-0.142	-35.20	-5.62
9	-2.59	2.90	-39.70	0.46	-2.54	2.90	-39.60	0.47
10	49.90	17.30	99.60	40.40	50.10	17.30	99.80	40.40

Note: L = 100 ft , E_b = 432,000 k/ft^2 , ν_b = 0.2 , ν_s = 0.2 .

APPENDIX B: VERTICAL DISPLACEMENTS AND TRACTIONS AT INTERFACE, CATEGORY 2

Table B1

Vertical Displacements at Interface, Loading Case 1

UDL 5 k/ft--Top of Beam

Detail	H/L = 1				H/L = 2			
	L/t = 10		L/t = 20		L/t = 10		L/t = 20	
	$n = E_b/E_s$		$n = E_b/E_s$		$n = E_b/E_s$		$n = E_b/E_s$	
	10	100	10	100	10	100	10	100
Case	1	2	3	4	5	6	7	8
	$\times 10^{-3}$	$\times 10^{-2}$	$\times 10^{-3}$	$\times 10^{-2}$	$\times 10^{-2}$	$\times 10^{-1}$	$\times 10^{-2}$	$\times 10^{-1}$
Node No.								
1	-8.888	-8.386	-9.173	-8.924	-1.266	-1.208	-1.306	-1.268
2	-8.862	-8.370	-9.147	-8.897	-1.264	-1.206	-1.303	-1.265
3	-8.783	-8.323	-9.066	-8.815	-1.255	-1.202	-1.294	-1.256
4	-8.651	-8.246	-8.929	-8.679	-1.241	-1.194	-1.279	-1.242
5	-8.468	-8.141	-8.731	-8.491	-1.221	-1.183	-1.256	-1.222
6	-8.236	-8.011	-8.467	-8.252	-1.197	-1.170	-1.227	-1.197
7	-7.960	-7.861	-8.131	-7.967	-1.168	-1.156	-1.190	-1.167
8	-7.649	-7.696	-7.721	-7.644	-1.136	-1.139	-1.146	-1.134
9	-7.316	-7.521	-7.249	-7.293	-1.103	-1.122	-1.097	-1.098
10	-6.968	-7.340	-6.745	-6.930	-1.070	-1.105	-1.046	-1.062
11	-6.683	-7.168	-6.294	-6.572	-1.045	-1.089	-1.004	-1.027

Note: L = 100 ft , E_b = 432,000 k/ft^2 , ν_b = 0.2 , ν_s = 0.2 .

Table B2

Vertical Tractions at Interface, Loading Case 1

UDL 5 k/ft--Top of Beam

Detail	H/L = 1				H/L = 2			
	L/t = 10		L/t = 20		L/t = 10		L/t = 20	
	$n = E_b/E_s$		$n = E_b/E_s$		$n = E_b/E_s$		$n = E_b/E_s$	
	10	100	10	100	10	100	10	100
Case	1	2	3	4	5	6	7	8
	$\times 10^1$	$\times 10^1$	$\times 10^1$	$\times 10^1$	$\times 10^1$	$\times 10^1$	$\times 10^1$	$\times 10^1$
Element No.								
1	-0.487	-4.330	-0.499	-0.492	-0.479	-0.421	-0.497	-0.485
2	-0.485	-4.320	-0.498	-0.489	-0.477	-0.420	-0.496	-0.483
3	-0.480	-4.310	-0.498	-0.484	-0.472	-0.419	-0.496	-0.478
4	-0.473	-4.290	-0.496	-0.477	-0.464	-0.419	-0.493	-0.471
5	-0.464	-4.280	-0.492	-0.467	-0.455	-0.421	-0.489	-0.462
6	-0.452	-4.300	-0.484	-0.456	-0.444	-0.426	-0.479	-0.452
7	-0.442	-4.400	-0.469	-0.447	-0.436	-0.441	-0.462	-0.445
8	-0.443	-4.680	-0.449	-0.446	-0.442	-0.476	-0.442	-0.449
9	-0.456	-5.250	-0.429	-0.465	-0.466	-0.543	-0.428	-0.478
10	-0.818	-9.830	-0.686	-0.776	-0.865	-1.010	-0.719	-0.798

Note: $L = 100$ ft , $E_b = 432{,}000$ k/ft^2 , $\nu_b = 0.2$, $\nu_s = 0.2$.

Table B3

Vertical Displacements at Interface, Loading Case 2

Point Load 250 k--Beam Ends

Detail	H/L = 1				H/L = 2			
	L/t = 10		L/t = 20		L/t = 10		L/t = 20	
	$n = E_b/E_s$		$n = E_b/E_s$		$n = E_b/E_s$		$n = E_b/E_s$	
	10	100	10	100	10	100	10	100
Case	1	2	3	4	5	6	7	8
	$\times 10^{-3}$	$\times 10^{-2}$	$\times 10^{-3}$	$\times 10^{-2}$	$\times 10^{-3}$	$\times 10^{-2}$	$\times 10^{-3}$	$\times 10^{-2}$
Node No.								
1	-3.584	-5.048	-3.424	-3.312	-7.387	-8.765	-7.25	-7.047
2	-3.643	-5.112	-3.460	-3.383	-7.443	-8.829	-7.282	-7.116
3	-3.826	-5.304	-3.568	-3.600	-7.619	-9.021	-7.381	-7.328
4	-4.151	-5.624	-3.757	-3.983	-7.935	-9.340	-7.554	-7.702
5	-4.653	-6.073	-4.050	-4.560	-8.423	-9.789	-7.825	-8.269
6	-5.379	-6.650	-4.497	-5.372	-9.136	-10.370	-8.246	-9.070
7	-6.396	-7.353	-5.215	-6.468	-10.140	-11.070	-8.934	-10.150
8	-7.791	-8.178	-6.437	-7.897	-11.530	-11.900	-10.130	-11.580
9	-9.683	-9.118	-8.618	-9.703	-13.420	-12.840	-12.290	-13.330
10	-12.020	-10.150	-12.380	-11.890	-15.780	-13.880	-16.050	-15.570
11	-14.660	-11.220	-18.100	-14.380	-18.450	-14.960	-21.800	-18.060

Note: L = 100 ft , E_b = 432,000 k/ft^2 , ν_b = 0.2 , ν_s = 0.2 .

Table B4

Vertical Tractions at Interface, Loading Case 2

Point Load 250 k--Beam Ends

Detail	H/L = 1				H/L = 2			
	L/t = 10		L/t = 20		L/t = 10		L/t = 20	
	$n = E_b/E_s$		$n = E_b/E_s$		$n = E_b/E_s$		$n = E_b/E_s$	
	10	100	10	100	10	100	10	100
Case	1	2	3	4	5	6	7	8
Element No.								
1	0.746	-0.197	0.062	1.150	0.818	-0.071	0.078	1.210
2	0.768	-0.328	0.109	1.130	0.843	-0.206	0.126	1.180
3	0.792	-0.600	0.227	1.050	0.871	-0.488	0.247	1.110
4	0.764	-1.040	0.465	0.847	-0.847	-0.940	0.491	0.905
5	0.578	-1.680	0.886	0.408	0.664	-1.610	0.921	0.463
6	0.042	-2.600	1.490	-0.464	0.126	-2.560	1.530	-0.420
7	-1.200	-3.920	2.030	-2.100	-1.140	-3.920	2.100	-2.080
8	-4.260	-5.980	1.090	-5.160	-4.250	-6.050	1.160	-5.190
9	-10.100	-9.090	-4.660	-10.400	-10.200	-9.280	-4.660	-10.600
10	-38.100	-24.600	-51.700	-36.400	-38.600	-24.900	-52.000	-36.600

Note: L = 100 ft , E_b = 432,000 k/ft^2 , ν_b = 0.2 , ν_s = 0.2 .

Table B5

Vertical Displacements at Interface, Loading Case 3

Moment of 5,000 ft-k--Beam Ends

Detail	H/L = 1				H/L = 2			
	L/t = 10		L/t = 20		L/t = 10		L/t = 20	
	$n = E_b/E_s$		$n = E_b/E_s$		$n = E_b/E_s$		$n = E_b/E_s$	
	10	100	10	100	10	100	10	100
Case	1	2	3	4	5	6	7	8
	$\times 10^{-3}$	$\times 10^{-2}$	$\times 10^{-3}$	$\times 10^{-2}$	$\times 10^{-3}$	$\times 10^{-2}$	$\times 10^{-3}$	$\times 10^{-2}$
Node No.								
1	-3.371	-2.809	-2.684	-3.990	-3.246	-2.769	-2.567	-3.961
2	-3.391	-2.758	-2.733	-3.997	-3.266	-2.719	-2.616	-3.968
3	-3.440	-2.605	-2.893	-4.004	-3.316	-2.565	-2.777	-3.975
4	-3.487	-2.340	-3.200	-3.970	-3.364	-2.301	-3.084	-3.941
5	-3.470	-1.953	-3.704	-3.820	-3.349	-1.914	-3.590	-3.792
6	-3.284	-1.423	-4.438	-3.440	-3.164	-1.385	-4.325	-3.411
7	-2.766	-0.732	-5.288	-2.661	-2.648	-0.694	-5.177	-2.632
8	-1.657	0.148	-5.751	-1.257	-1.541	0.186	-5.643	-1.229
9	0.658	1.270	-4.267	1.066	0.773	1.307	-4.161	1.093
10	4.950	2.691	3.580	4.751	5.064	2.729	3.685	4.778
11	10.660	4.292	22.890	9.937	10.780	4.329	22.990	9.963

Note: L = 100 ft, $E_b = 432{,}000\ k/ft^2$, $\nu_b = 0.2$, $\nu_s = 0.2$.

Table B6

Vertical Tractions at Interface, Loading Case 3

Moment of 5,000 ft-k--Beam Ends

Detail	H/L = 1				H/L = 2			
	L/t = 10		L/t = 20		L/t = 10		L/t = 20	
	$n = E_b/E_s$		$n = E_b/E_s$		$n = E_b/E_s$		$n = E_b/E_s$	
	10	100	10	100	10	100	1C	100
Case	1	2	3	4	5	6	7	8
Element No.								
1	-1.97	-3.16	0.01	-2.90	-1.98	-3.17	0.01	-2.90
2	-2.30	-3.14	-0.07	-3.23	-2.31	-3.14	-0.07	-3.23
3	-2.98	-3.07	-0.36	-3.85	-2.98	-3.07	-0.36	-3.85
4	-4.01	-2.94	-1.19	-4.72	-4.01	-2.94	-1.19	-4.72
5	-5.36	-2.69	-3.22	-5.72	-5.37	-2.69	-3.23	-5.72
6	-6.94	-2.25	-7.53	-6.57	-6.95	-2.25	-7.54	-6.57
7	-8.74	-1.52	-15.60	-6.76	-8.75	-1.52	-15.60	-6.77
8	-8.96	-0.13	-28.30	-5.25	-8.96	-0.13	-28.30	-5.25
9	-1.79	2.71	-33.50	0.41	-1.79	2.71	-33.60	0.40
10	43.10	16.20	89.90	38.60	43.10	16.20	89.90	38.60

Note: L = 100 ft , E_b = [illegible] , $\nu_b = 0.2$, $\nu_s = 0.2$.

APPENDIX C: FINITE-ELEMENT STUDY RESULLTS FOR CASES 5, 6, 7, AND 8

Table C1

Vertical Displacements at Interface, Loading Case 1

UDL 5 k/ft--Top of Beam

Detail	H/L = 2			
	L/t = 10		L/t = 20	
	$n = E_b/E_s$		$n = E_b/E_s$	
	10	100	10	100
Case	5	6	7	8
	$\times 10^{-2}$	$\times 10^{-1}$	$\times 10^{-2}$	$\times 10^{-1}$
Node No.				
1	-1.320	-1.256	-1.363	-1.322
2	-1.318	-1.254	-1.360	-1.319
3	-1.309	-1.248	-1.350	-1.310
4	-1.294	-1.240	-1.335	-1.294
5	-1.273	-1.227	-1.312	-1.273
6	-1.247	-1.212	-1.282	-1.246
7	-1.216	-1.195	-1.244	-1.213
8	-1.180	-1.176	-1.198	-1.176
9	-1.142	-1.155	-1.143	-1.136
10	-1.103	-1.134	-1.083	-1.093
11	-1.063	-1.113	-1.023	-1.050

Note: $L = 100$ ft, $E_b = 432{,}000$ k/ft^2, $\nu_b = 0.2$, $\nu_s = 0.2$.

APPENDIX C: FINITE-ELEMENT STUDY RESULLTS FOR CASES 5, 6, 7, AND 8

Table C3

Vertical Displacements at Interface, Loading Case 2

Point Load of 250k--Beam Ends

Detail	H/L = 2			
	L/t = 10		L/t = 20	
	$n = E_b/E_s$		$n = E_b/E_s$	
	10	100	10	100
Case	5	6	7	8
	$\times 10^{-3}$	$\times 10^{-2}$	$\times 10^{-3}$	$\times 10^{-2}$
Node No.				
1	-8.006	-9.238	-7.830	-7.732
2	-8.060	-9.295	-7.864	-7.795
3	-8.225	-9.467	-7.970	-7.987
4	-8.518	-9.755	-8.158	-8.324
5	-8.964	-10.160	-8.450	-8.827
6	-9.603	-10.680	-8.891	-9.527
7	-10.490	-11.300	-9.570	-10.460
8	-11.680	-12.040	-10.640	-11.660
9	-13.280	-12.880	-12.360	-13.150
10	-15.300	-13.810	-15.210	-14.950
11	-17.010	-14.730	-18.630	-16.910

Note: L = 100 ft , $E_b = 432,000\ k/ft^2$, $\nu_b = 0.2$, $\nu_s = 0.2$.

Table C2

Vertical Displacements at Interface, Loading Case 3

Moment of 5,000 ft-k--Beam Ends

Detail	H/L = 2			
	L/t = 10		L/t = 20	
	$n = E_b/E_s$		$n = E_b/E_s$	
	10	100	10	100
Case	5	6	7	8
	$\times 10^{-3}$	$\times 10^{-2}$	$\times 10^{-3}$	$\times 10^{-2}$
Node No.				
1	-3.149	-2.771	-2.544	-3.757
2	-3.169	-2.725	-2.590	-3.768
3	-3.223	-2.585	-2.738	-3.791
4	-3.283	-2.343	-3.016	-3.790
5	-3.297	-1.988	-3.465	-3.701
6	-3.175	-1.502	-4.114	-3.423
7	-2.780	-0.865	-4.883	-2.810
8	-1.880	-0.051	-5.416	-1.166
9	0.082	0.992	-4.633	0.289
10	3.937	2.327	1.350	3.476
11	8.211	3.799	14.620	7.975

Note: L = 100 ft , E_b = 432,000 k/ft^2 , ν_b = 0.2 , ν_s = 0.2 .

APPENDIX D: NOTATION

b_i	Body force vector
C_{ijkl}	Fourth-order material property tensor
E_b	432,000 k/ft^2, modulus of elasticity of beam
f_B	Condensed force vector representing prescribed forces and displacements on the boundary of the soil medium
F_B	Forces in beam
F_S	Forces on soil
[G] and [H]	Square matrices of the order $2 \times m$
k	Proportionality constant, known as the subgrade modulus or the modulus of subgrade reaction
$[k_B]$	Condensed stiffness matrix to represent soil
K_{BB}	Beam stiffness
K_{SB}, K_{BS}	Off-diagonal stiffness beams
K_{SS}	Soil stiffness
L	Length of beam
M	Total number of boundary elements
n	Unit normal vector on the boundary
p	Pressure acting on the soil surface
q	Field point where the displacements and tractions are calculated due to the unit load
$r = r(s,q)$	Distance between the load point s and field point q
s	Source point where a unit load is applied in the specified direction
$\tilde{t}_i$	Prescribed tractions on boundary
t^*_{il}	Tractions in the i direction due to a unit concentrated load at s in the l direction
[T]	Transformation matrix which converts finite-element displacements of interface nodes into the boundary-element displacement at the midpoints
T_i	Tractions in element i
T^n_j	Nodal values of traction vectors on the n^{th} boundary element
T_B	Traction vector
u^*_i	Assumed weighting function
u^*_{il}	Displacements in the i direction due to a unit concentrated load at s in the l direction
U^b and F^b	Nodal displacements at midpoints of the boundary elements at the interface

U_j	Displacement in element j
U_j^n	Nodal values of displacement on the n^{th} boundary element
U_B	Beam displacements
U_S	Soil displacements
V_P and V_U	Vectors representing the prescribed and the unknown components of all displacements and tractions on boundaries g_1, g_2, and g_3
w	Deflection of the loaded region on the surface
Γ	Complete exterior boundary
Γ_m	Boundary for m^{th} element
Γ_r	Exterior boundary except for Γ_E
Γ_E	Circular augmented surface at source point for radius (r) equal to some assumed error (ϵ)
Γ_1	Exterior boundary where tractions are prescribed
Γ_2	Exterior boundary where displacements are prescribed
ϵ_{ij}	Linear strain tensor
σ_{ij}	Stress tensor
ν_b	0.2, Poisson's ratio of beam
ν_s	0.2, Poisson's ratio of soil
ϕ_{ij} and ψ_{ij}	Interpolation functions
Ω	Interior domain of a solid continuum

END
DTIC
8-86